Synthesis and characterisation of hybrid graft copolymers of polydimethylsiloxane and polymethylmethacrylate

by

Gretha Krügel

Thesis is presented in partial fulfillment of the requirements for the degree of Master of Science at the University of Stellenbosch

Study Leader
Dr. PE Mallon

Stellenbosch
October 2007

I, the undersigned, hereby declare that the work contained in this thesis is my original work and that I have not previously in its entirety or in part submitted it at any university for a degree.

Signature:……..

Date:…….

Abstract

Hybrid graft copolymers of polydimethylsiloxane (PDMS) and polymethylmethacrylate (PMMA) were synthesised. PDMS macromonomers were synthesised anionically from the cyclic D_3 monomer. This living polymerisation was terminated with a [3-(methacryloxy)propyl]-dimethylchlorosilane terminating agent which resulted in the functionalised macromonomer. These PDMS macromonomers and MMA monomer were copolymerised to form PMMA-g-PDMS hybrid copolymers by conventional free radical reactions. Synthesised and commercial methacryloxy-functionalised PDMS macromonomers having a range of molar masses were copolymerised with MMA to form graft copolymers of various chemical compositions. PDMS content in the graft copolymers could be varied by the amount of PDMS incorporated into the copolymer as well as by varying the length of the PDMS side chains. Size exclusion chromatography (SEC) results confirmed low PDI's for the PDMS macromonomers synthesised anionically. NMR studies allowed characterisation of the synthesised PDMS macromonomers and PMMA-g-PDMS copolymers. It also allowed the determination of relative ratios of PMMA:PDMS in the graft copolymers. Gradient elution chromatography (GEC) was used successfully to monitor the presence and removal of the PDMS macromonomer from the graft copolymer products. The influence of PDMS content of the graft copolymers on retention time was also evaluated using this technique. Two dimensional chromatography confirmed the formation of PMMA-g-PDMS copolymer as well as PMMA homopolymer during some of the grafting reactions. GEC in the first dimension was coupled to SEC in the second dimension. PAS-FTIR studies allowed chemical characterisation of the graft copolymer and confirmed surface segregation of the PDMS. Atomic force microscopy (AFM) was also used to study the surface segregation of PDMS and looked at the relationship between surface polarity and increasing PDMS content. The study showed the effect of thermal treatment on the surface morphology of the hybrid polymers. Corona treatment was used to modify the surface structure of the graft copolymer films. Contact angle studies provided evidence of hydrophobic loss and recovery after corona for the hybrid polymer materials containing PDMS. This is one of the first reported examples of hydrophobicity recovery in these types of hybrid materials after corona treatment. Slow positron beam studies highlighted the formation of a thin silica like layer on the surface of the films after corona similar to that observed for pure cross-linked PDMS compounds. The positron studies enabled estimation of the thickness of the silica like layer.

Opsomming

Hibried ent kopolimere van polidimetielsiloksaan (PDMS) en polimetielmetakrilaat (PMMA) is gesintetiseer. PDMS makromonomere is anionies gesintetiseer van die sikliese D_3 monomeer. Die lewende polimerisasie is getermineer met ‘n [3-(metakriloksie) propiel]-dimetielchlorosilaan termineringsagent wat gelei het tot die vorming van die funksionele makromonomeer. Hierdie PDMS makromonomere en MMA monomeer is geko-polimeriseer om PMMA-g-PDMS hibried ko-polimere te vorm deur konvensionele vrye radikaal reaksies. Gesintetiseerde en kommersiële metakriloksie-funksionele PDMS makromonomere met ‘n reeks verskillende molêre massas is geko-polimeriseer met MMA om ent ko-polimere te vorm met verskeie chemiese komposisies. PDMS inhoud in die ent ko-polimere is gevarieer deur die hoeveelheid inkorporasie van PDMS in die kopolimeer asook deur variasie in die lengte van die PDMS sy-kettings. Grootte uitsluitings chromatografie (GUC) resultate wys dat lae polidispersie indeks (PDI) PDMS makromonomere anionies gesintetiseer is. Kern magnetiese resonansie spektroskopie (KMR) studies laat die karakterisering van PDMS makromonomere en PMMA-g-PDMS ko-polimere toe. Dit lei ook tot die bepaling van die relatiewe verhouding van PMMA:PDMS in die ko-polimere. Gradiënt-vloeistof chromatografie (GVC) is suksesvol gebruik om die teenwoordigheid en verwydering van die PDMS makromonomeer in die ko-polimeer produkte te monitor. Die invloed van die PDMS inhoud van die ko-polimere op retensie tyd is ook geëvalueer deur hierdie tegniek. Twee-dimensionele chromatografie bevestig die vorming van PMMA-g-PDMS ko-polimeer asook PMMA homopolimeer tydens sommige van die ko-polimerisasie reaksies. GVC in die eerste dimensie is gekoppel aan GUC in die tweede dimensie. Foto-akoestiese fourier transform infrarooi (PAS-FTIR) studies lei tot die chemiese karakterisering van die ent ko-polimere en bevestig oppervlak segregasie van die PDMS. Atomiese krag mikroskopie (AKM) is ook gebruik om die oppervlak segregasie van PDMS te bestudeer en daar is ook gekyk na die verhouding tussen oppervlak polariteit en toenemende PDMS inhoud. Die studie dui op die effek van hitte behandeling op die oppervlak morfologie van die hibried ko-polimere. Korona behandeling is gebruik om die oppervlak struktuur van die ent ko-polimere te modifiseer. Kontak hoek studies bewys verlies en herstel van hidrofobisiteit van die hibried polimeer materiaal na korona behandeling. Hierdie is die eerste voorbeeld van herstel van hidrofobisiteit van hierdie tipe hibried materiale na korona behandeling. Stadige positronstraal studies dui op die vorming van ‘n dun silika-tipe lagie op die oppervlak van

die films na korona behandeling soortgelyk aan die resultate van suiwer PDMS materiale. Die positron studies vergemaklik die benaderde bepaling van die diktheid van die silika-tipe lagie.

Acknowledgements

Firstly, I would like to thank my promoter Dr Peter Mallon for all the guidance and support during this project.

I would like to thank the following people for analysing my samples. Jean McKenzie and Elsa Malherbe for their help with NMR analysis. Thanks to Dr Valerie Grumel for assistance with the analysis on the HPLC and GPC instruments. Thanks to Roediger Agencies for PAS-FTIR analysis as well as use of instruments for static contact angle measurements. Martina Meincken for assistance with the AFM analysis of samples. I would also like to thank Prof. Y.C. Jean from the University of Missouri, Kansas City for arranging use of the instrument for slow positron beam analysis.

Thanks to all the staff at the department of polymer science, Calvin, Adam, Hennie, Aneli and Erinda for their help.

The NRF is thanked for bursary funding during this research project.

Thanks to all my lab-mates in Lab 134, especially Gareth Bayley for all the help during this project. Thanks to everyone at Deetlefs that gave me the opportunity to finish this project.

I would like to thank my parents and the rest of my family for all their support and last but not least, a special thanks to Dawid for all the support, patience and understanding.

List of Contents

Chapter 3: Experimental

Chapter 4: Results and Discussion

Chapter 5: Conclusions and Recommendations

List of Figures

Chapter 2

Chapter 3

Chapter 4

List of Tables

Chapter 3

Chapter 4

List of Schemes

Chapter 2

Chapter 4

Glossary

Abbreviations

AFM	Atomic Force Microscopy
ATH	alumina trihydrate
AIBN	2,2'-azobis(isobutyronitrile)
BuLi	butyllithium
CCD	chemical composition distribution
CRP	controlled radical polymerisation
C_s	transfer constant for transfer agent S
D_3	hexamethylcyclotrisiloxane
DBES	Doppler broadening of energy spectra
DPFM	digital pulsed force mode
DRI	differential refractive index
ELSD	evaporative light scattering detector
EPDM	ethylene propylene diene monomer
FTIR	Fourier Transform Infra-Red
GEC	Gradient Elution Chromatography
GPC	Gel Permeation Chromatography
Homo-PDMS	polydimethylsiloxane homopolymer
HPLC	High-Performance Liquid Chromatography
IOP	inorganic-organic polymers
KOH	potassium hydroxide
LCCC	Liquid Chromatography at Critical Conditions
LDA	lithium diisoprolyamide
LiCl	lithium chloride salt
LMW	low molecular weight
MeOH	methanol
$MgSO_4$	magnesium sulphate
MM	molar mass
MMA	methyl methacrylate
MMD	molar mass distribution
MMP-PDMS	monomethacryloxypropyl terminated polydimethylsiloxane
M_n	number average molar mass

MPDC	[3-(methacryloxy)propyl]-dimethylchlorosilane
M_w	weight average molar mass
N_2	nitrogen
NMR	Nuclear Magnetic Resonance
NP	normal phase column
OIP	organic-inorganic polymers
OM	Optical Microscopy
PAL	Positron Annihilation Lifetime Spectroscopy
PAS	Positron Annihilation Spectroscopy
PAS-FTIR	Photo-Acoustic Scanning Fourier Transform Infrared
PDI	polydispersity index
PDMS	poly(dimethylsiloxane)
PMMA	poly(methyl methacrylate)
PS	polystyrene
Ps	positronium
RI	refractive index
RP	reversed phase column
SEC	Size Exclusion Chromatography
SEM	Scanning Electron Microscopy
SLM	standard liter per minute
SPM	Scanning Probe Microscopy
STM	Scanning Tunneling Microscopy
TEM	Transmission Electron Microscopy
Tg	glass transition temperature
THF	tetrahydrofuran
UV	ultraviolet

Symbols

[A]	comonomer concentration
E_+	incident energy
f_a	molar proportion of A in monomer mixture
F_a	mole percentage of A units in copolymer
$[I]_o$	initial initiator concentration
k	rate constant
[M]	macromonomer concentration
M_o	initial monomer concentration
P_{aa}	possibility to find diad AA
r	reactivity ratio
S	S parameter
x	fractional conversion
Z	depth penetration

Chapter 1

General Introduction and objectives

1.1 General Introduction

Hybrid polymers are gaining special interest in the attempts by scientists to create specialised, high performance materials from existing monomers. Hybrid materials consist of organic and inorganic segments. These copolymers are of great interest because inorganic polymers generally have unique and specific properties that organic polymers do not show. By combining these segments in hybrid copolymers, the polymer combines the properties of the disparate components. The hybrid polymers under study in this project are poly (methyl methacrylate)-graft-polydimethylsiloxane (PMMA-g-PDMS) copolymers and the two components have very dissimilar properties. Even at high molecular weight PDMS is a viscous liquid at room temperature, while PMMA is a glassy, brittle material. Hybrid polymers can have a wide range of architectural structures, namely block copolymers (di-blocks and tri-blocks), graft copolymers and star copolymers. Polymerisation techniques that allow control over all of these factors need to be utilised in the process of creating these complex molecular architectures. These polymerisation techniques range from the more recently developed controlled radical polymerisation techniques like atom transfer radical polymerisation (ATRP)[1], reversible addition fragmentation chain transfer polymerisation (RAFT)[2] and nitroxide mediated polymerisation (NMP)[3] to the first living polymerisation technique, namely anionic polymerisation[4]. Without these techniques, the synthesis of complex hybrid polymers with controlled structure would not be possible.

Complex hybrid polymers, like the graft copolymer studied in this project, require advanced analytical techniques. Liquid chromatography has been established as a primary technique to analyse and characterise heterogeneous polymeric materials[5]. Complex copolymers are distributed in chemical composition and molecular mass and these techniques should allow characterisation of these properties. The two main liquid chromatographic techniques that have been developed to monitor the chemical composition of complex polymer systems are gradient elution chromatography and chromatography under the critical conditions of one or other of the copolymer

components. Two dimensional chromatography techniques have also been developed where size exclusion chromatography is used in the second dimension to determine both the chemical composition distribution and the molar mass distribution. This allows for the total characterisation of polymers in more than one distributive property. These advanced chromatographic techniques will be used and developed to investigate the nature of the various graft copolymers synthesised in this project.

Pure cross-linked PDMS materials are used in many applications including as materials for the sheds in high voltage electrical insulators. One of the main reasons for this is the hydrophobic nature of the PDMS material. A second important reason for their use is the fact that these materials have the ability to undergo a hydrophobicity recovery process after electrical discharge (for example corona discharge) has occurred on the surface. A number of important studies of this process have been done using various analytical techniques including S parameter measurements by the slow positron beam by Mallon *et al*.[6] to show a systematic change in S parameter as a function of corona treatment time for pure PDMS compounds. Evidence for the diffusion of LMW PDMS (formed during discharge) back to the surface was found in the S parameter curves by Mallon *et al*[7]. Bayley *et al*.[8] has recently shown that polystyrene-block-PDMS copolymers also show this hydrophobicity recovery phenomenon.

So far no studies have been done on PDMS based hybrid materials in terms of their behaviour in response to corona discharge. This study aims to firstly synthesise PDMS based graft materials, evaluate the preferential surface segregation of the PDMS component, and examine if these materials will show a similar response to corona treatment as pure cross-linked PDMS compounds.

1.2 Objectives

The main objectives of this research project were as follows.

- Evaluation of the synthesis of methacryloxy functionalised PDMS macromonomers formed via anionic polymerisation of D_3 monomer by (methacryloxy)propyl-dimethylchlorosilane termination.

- Evaluation of the synthesis of hybrid PMMA-graft-PDMS copolymers formed during conventional free radical polymerisation of PDMS macromonomer with MMA illustrating the ‘grafting through’ technique.
- Synthesis of a series of PMMA-g-PDMS copolymers with various PDMS content by variation of the graft density as well as the graft lengths.
- The development of a GEC profile to allow monitoring of the presence and removal of PDMS macromonomer after copolymerisation.
- The development of two dimensional chromatography techniques by the coupling of GEC to SEC for two dimensional analyses to confirm formation of PMMA-g-PDMS and PMMA homopolymer.
- The evaluation of PDMS surface segregation using various analytical techniques.
- The evaluation of hydrophobicity loss and recovery after corona treatment using static contact angle measurements.
- The evaluation of the surface modification after corona treatment using the slow positron beam.

1.3 References

(1) Greszta, D.; Mardare, D.; Matyjaszewski, K. *Macromolecules* **1994**, *27*, 638-644.

(2) Chiefari, J.; Chong, Y. K.; Ercole, F.; Krstina, J.; Jeffery, J.; Le, T. P. T.; Mayadunne, R. T. A.; Meijs, G. F.; Moad, C. L.; Moad, G.; Rizzardo, E.; Thang, S. H. *Macromolecules* **1998**, *31*, 5559-5562.

(3) George, M. K.; Veregin, R. P. N.; Kazmaier, P. M.; Hamer, G. K. *Macromolecules* **1993**, *26*, 2987-2988.

(4) Hong, K.; Uhrig, D.; Mays, J. W. *Curr. Opin. Solid State Mater. Sci.* **1999**, *4*, 531-538.

(5) Pasch, H.; Trathnigg, B. *HPLC of polymers*; Springer: Berlin-Heidelberg-New York, 1998.

(6) Mallon, P. E.; Berhane, T. A.; Greyling, C. J.; Vosloo, W. L.; Chen, H.; Jean, Y. C. *Mater. Sci. Forum* **2004**, *445-446*, 322-324.

(7) Mallon, P. E.; Greyling, C. J.; Vosloo, W.; Jean, Y. C. *Radiat. Phys. Chem.* **2003**, *68*, 453-456.

(8) Bayley, G.; Mallon, P. E. *Polym. Eng. Sci.* **2007**, *article in press*.

Chapter 2

Historical Overview

2.1 Hybrid polymers

The possibilities for producing new monomers at low cost have been decreasing; therefore many scientists are striving to create specialised, high performance materials from existing monomers by synthesising copolymers of various architectures and compositions. One set of copolymers that are gaining special interest is hybrid polymers. By using different combinations of organic and inorganic components, a wide range of polymeric structures have been synthesised via controlled radical polymerisation (CRP) by Pyun *et al*[1].

There are two main types of hybrid polymers, namely, organic-inorganic polymers (OIP) and inorganic-organic polymers (IOP). The former material consists of an organic backbone with inorganic side chains and the latter has an inorganic backbone with organic pendant chains. These copolymers are of such interest because inorganic polymers generally have unique and specific properties that organic polymers do not have[2].

In this study, we will focus on graft copolymers, namely PMMA-graft-PDMS copolymers. The incorporation of microphase-separated polydimethylsiloxane (PDMS) domains into a polymethylmethacrylate (PMMA) matrix allows the system to show many of the desirable properties of both components. The properties of both components are shown due to their severe incompatibility and this makes these types of copolymers of such high interest. Some of the desirable properties of the PMMA matrix are very good optical clarity, good UV stability, high electrical resistivity and hydrolytic stability[3]. A key property of PDMS is its low surface energy, which results in surface segregation of PDMS in most polymer blend systems. Polysiloxanes and their copolymers have very interesting properties such as elastomeric behavior; good thermal, UV and oxidative stabilities; good weatherability; low surface energy; high gas permeability and biocompatibility[4]. PDMS also has interesting properties when exposed to corona discharges as shown by Mallon *et al*[5].

2.2 Graft copolymers

There are a large number of possible architectures for hybrid polymers. In this study we will focus on graft copolymers. Graft copolymers show good phase separation and are used for a variety of applications, such as impact-resistant plastics, thermoplastic elastomers, compatibilisers and polymeric emulsifiers. They generally have lower melt viscosities because of their branched structure, which is advantageous for processing. Since graft copolymers have so many structural variables (branch length, branch spacing, backbone length, composition and many more), they have great potential to realise new properties[2].

Graft copolymers are macromolecules with a main chain or backbone composed of one type of polymer and side chains or grafts of another polymer. The physical and chemical properties of graft copolymers can be tailored to suit various applications by choice of the different chemical compositions of the backbone and side chains. Most approaches for the synthesis of graft copolymers fall into one of three main categories: 'grafting onto', 'grafting from', and the macromonomer technique, also called 'grafting through'. A summary of these three main techniques[6] will be given below to better explain the mechanism and advantages of each. These three grafting techniques are illustrated in figure 2.1.

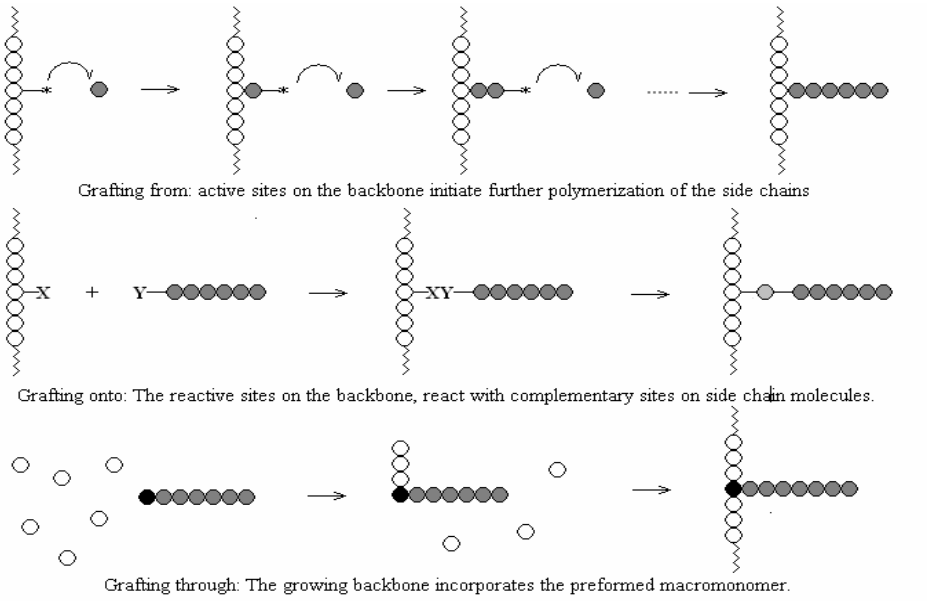

Figure 2.1: The three main grafting techniques.

2.3 Grafting techniques

2.3.1 'Grafting onto'

In the grafting onto technique both the side chains and the backbone are pre-polymerised before the grafting event. The functional ends of the side chains are covalently bonded with complementary functionalities along the backbone. Therefore there is a reaction between the electrophilic sites along the main chain with nucleophilic chain ends of the living side chains. This implies that access of the functional chain end to the grafting sites is permitted. This is not always easy, due to the known incompatibility between polymers of different chemical natures. One common procedure utlises chloromethylation of polystyrene[6,7]. Chloromethyl groups couple well with oxyanions, but coupling with stronger nucleophiles can lead to undesirable lithium-halogen exchange reactions. Rahlwes *et al*.[8] overcame these side reactions by the conversion of chloromethyl groups into chlorosilyl moieties, making well-defined poly(styrene-graft-isoprene) copolymers. The ease of sampling of both the side chains and backbone for characterisation are the main advantage of this technique[9]. This also allows for the structural characterisation of the graft copolymer formed.

2.3.2 'Grafting from'

In this technique only the backbone is pre-polymerised prior to the grafting event. The side chains are then polymerised from the backbone which serves as the multi-initiation site. Grafting from by anionic polymerisation employs acid/base chemistry[10-12]. Acidic hydrogens on phenol[10], alcohol or amide[12] may be removed and result in ethylene oxide polymerisation. Hydrogens that are α to a carbonyl group are acidic enough to be removed by lithium diisoprolyamide (LDA) and the generated anions are suited to initiate methacrylic monomers[11]. The backbone can have a multitude of sites reactive enough to initiate an anionically polymerisable monomer. The creating of reactive sites along the backbone by irradiation[10] or chemical treatment[13], followed by addition of a monomer to generate a graft copolymer, makes this technique a more expedient process than 'grafting onto' and therefore makes this an industrially important and advantageous grafting method.

2.3.3 'Grafting through'

We will focus on the 'grafting through' or macromonomer technique which employs a preformed side chain that has a polymerisable group at one end of the chain and is called a macromonomer. Grafting occurs by simply polymerising a monomer in the presence of this macromonomer[9]. The backbone is basically 'sewn' through the ends of the prepolymerised side chains in the grafting process. A relative large number of different macromonomers are available with easily polymerisable terminal groups, allowing access to a wide range of copolymer compositions. The macromonomer branches can also be thoroughly characterised.

Macromonomers allow control of the number of grafts per copolymer macromolecule through choice of the reaction mixture ratio of macromonomer to monomer in the polymerisation reaction mixture. Macromoners of well-defined chain length, molecular mass distribution and terminal functionality can be obtained by the use of living polymerisation techniques[9]. A more detailed discussion of macromonomers and their reactions follows.

2.4 Macromonomers

Macromonomers are linear macromolecules of low molecular mass (10^3 – 10^4 g.mol^{-1}), carrying at their chain end some polymerisable functionality[14,15]. This functionality is an unsaturation in most cases, but it can also be an oxirane ring or another heterocycle that can undergo polymerisation. Polymerisation of bifunctional macromonomers results in the formation of network structures. Polymer chains having two functions at one chain end can also be referred to as a macromonomer and can participate in a step-growth process. These macromonomers should not be confused with telechelic polymers which have two functions at their chain ends. Macromonomers are of such interest, because they give easy access to a range of graft copolymers[16]. There are a wide range of reactions for the synthesis of macromonomers and a review[17] of some of the most important techniques that will also be applicable to this project is given below.

2.4.1 Macromonomer synthesis by anionic polymerisation methods

The major advantage of these methods is the living character of the polymer[18,19]. Anionic polymerisations are characterised by the long lifetime of the carbanionic sites[20,21]. When neither transfer nor termination reactions occur, the polymers show a narrow molecular weight distribution or polydispersity, provided initiation is fast compared to propagation. The number average degree of polymerisation is determined by the [monomer]/[initiator] molar ratio[16]. After polymerisation the active sites retain their reactivity and can be easily functionalised or end capped. End-capping is basically the deactivation of living polymeric anions by reacting it with an unsaturated electrophile. The deactivation must however be predominant to the attack of the unsaturation by carbanions. The most commonly used electrophiles include esters and organic halides[14,22,23] . The use of electrophiles is not always a fast method and can result in undesirable side reactions.

Several unsaturated electrophiles can be used in the end-capping of macromonomer synthesis. Firstly we have allyl halides[24] which could result in unwanted side reactions and are not very reactive in free-radical polymerisations. Benzyl halides[25] are efficient deactivators for living polystyrene, though the reaction competes with a side reaction involving attack of the carbanion at the double bond. No side reactions are detected when the reaction mixture contains tetrahydrofuran (THF). A disadvantage of this technique is the extreme sensitivity to contaminants like oxygen and moisture, which makes this a practically difficult technique to use.

Lutz and co-workers[26] have synthesised a polyalkylmethacrylate macromonomer anionically by the direct deactivation of the carbanionic sites with p-vinyl- or p-isopropenylbenzyl bromide. Three-armed-star-branched polymers were synthesised via the anionic synthesis of ω-1,1-diphenylethylene-terminated polystyrene macromonomers by Quirk *et al*[27]. Ishizu *et al.*[28] synthesised functionalised poly(ethylene oxide) macromonomers which can be applied for the synthesis of peripheral functionalised stars and polymer brushes as the starting materials. These functionalised poly(ethylene oxide) (PEO) macromonomers were prepared by ring-opening polymerisation of living PEO anions.

2.4.2 Macromonomer synthesis by cationic methods

Cationic polymerisation[29] will further be divided into two groups; heterocyclic monomers and vinylic monomers, since the mechanism for these two types of monomers differ so much. Some heterocyclic monomers might produce living cationic species where olefinic and vinylic monomers do not.

2.4.2.1 Heterocyclic monomers

Cationic ring-opening of some heterocycles, for instance oxolane are free of spontaneous termination and without transfer to monomer[30,31]. The lifetime of the active sites is long and the polymers are living. It must be taken into account that propagation is a reversible process and that the polydispersity tends to broaden when the ceiling temperature is approached. For efficient initiation, the cationic species should add to the monomer and associate to stable counterions. These living polymeric cations can also be end-capped. A functionalised end group is formed when an unsaturated nucleophile is used to deactivate the cation.

2.4.2.2 Vinylic monomers

The cationic polymerisation of vinyl monomers such as isobutene, styrene and vinyl ethers could be hindered by several transfer reactions. The methods that are based on the long lifetime of the active sites at the chain ends can not be applied here, since the molecular weight of the polymer is not determined by the molar ratio of monomer to initiator. The ‘inifer’ method[32,33] is to kinetically favor transfer to the initiator species in respect to transfer to any other species. The same species acts as initiator and transfer agent in these ‘inifer’ type reactions. Transfer to the monomer is negligible in these types of systems. Theoretically, the average molecular weight results from the ratio of the propagation rate to the rate of transfer; experimentally it results from the monomer-to-inifer mole ratio. ‘Inifer’ type reactions have been applied to a wide range of cationic synthesis, yielding functional polymers[34-36], block copolymers[37], graft copolymers and even star-shaped polymers[37].

2.4.3 Other two-step methods for the synthesis of macromonomers

The most commonly used method to synthesize macromonomers is still by the reaction of an unsaturated compound with an antagonist function located at the polymer chain end. In the next section we shall discuss the synthesis of polymers, where some kind of control of the molecular weight is formed. These polymers can then serve as precursors for macromonomer synthesis.

2.4.3.1 Step polymerisation

The self-polycondensation of molecules bearing two antagonist functions[38-40] at the chain ends (A-B), leads to the formation of a polymer that has different functionalities at the chain ends (A at the one end and B at the other). The syntheses of macromonomers are possible if one of these functions is reacted with an unsaturated compound. This self-condensation is the only type of self-condensation where the macromonomer is formed directly, without any additional reactions. The final species always carries an unsaturation at one chain end.

2.4.3.2 Free radical polymerisation

The active sites have a very short lifetime in this technique[41-46]. Therefore, functionalisation can arise only from the use of functional initiators or from transfer processes.

2.4.3.2 (i) Functional initiators

Homolytic cleavage results in a radical carrying the specific function. This functional group remains attached to the formed polymer molecule, since the primary radical ads to a monomer upon initiation. Functionalisation at only one chain end requires that termination occurs solely by disproportionation, not recombination. If this condition is not fulfilled, functionalisation at both chain ends can result. Transfer of the radical to monomer and solvent molecules can result in only a fraction of the formed macromolecules being functionalised. In addition there is a lack in control over the molecular weights of polymers. Low molecular weight species can only be obtained via

transfer reactions. Some initiators can act as transfer agents as well. It is possible to lower the molecular weight and have control over it by carrying out the polymerisation in the presence of a large amount of initiator; however, this leads to both chain ends being functionalised since it increases the probability of termination by coupling[47]. This method has many drawbacks and is not readily used in the synthesis of macromonomers.

2.4.3.2 (ii) Transfer reactions

The main function of a transfer agent is the control of the molecular weight of the species formed by a proper choice of the molar ratio [monomer]/[transfer agent] in a free-radical copolymerisation[48]. The efficiency of a transfer agent is given by its transfer constant C_s for the transfer agent S. The limiting degree of polymerisation is given by the ratio of the propagation rate to the rate of transfer, if the transfer agent is present in a sufficiently large amount and very effective. Broadening in the molecular weight distribution can be prevented by avoiding large changes in the molar ratio of monomer to transfer agent. Functional transfer agents can lead to the functionalisation of only one chain end. The transfer agent must allow functionalisation and control the molecular weight. A high value for C_s is important, since it minimises the amount of polymer produced by primary radicals. A low amount of polymer devoid of a terminal function is obtained if the occurrence of a transfer reaction is high.

2.4.3.2 (iii) Telomerisation

Telomerisation is a special case of free-radical transfer reactions. Monomers, such as vinyl chloride, vinylidene chloride and fluorine-containing monomers are of special interest here. Free-radical initiators, such as benzoyl peroxide, azo-bis-isobutyronitrile (AIBN) or redox processes[49,50] can be used to initiate telomerisation. Free-radical and redox systems differ greatly in this respect[51]. Macromolecules of high molecular weights are obtained by using free-radical initiation methods. Proper choice of reaction temperature, as well as the molar ratio of monomer to telogen, allows control over the molecular weight. It is easier to obtain adducts or well-defined oligomers using redox systems. Functional telogens are used to produce functional polymers, which are then reacted with unsaturated reagents to produce the terminal functionalised molecules[52].

2.5 Copolymerisation of macromonomers with comonomers

The major field of application of macromonomers is still the free-radical copolymerisation of a macromonomer with an acrylic or vinylic comonomer, since it leads to easy access of graft copolymers[53-56].

2.5.1 Fundamental theory

The general rules of copolymerisation are also applicable in the case of the copolymerisation of macromonomer with comonomer. The radical reactivity ratios (r) determine the ability of any of the two polymerisable species present to participate in the reaction. If the macromonomer is detonated by M and the comonomer by A, the well-known composition law applies to the copolymer that is formed[9]:

$$\frac{d[A]}{d[M]} = \frac{[A]}{[M]} \frac{r_a[A]+[M]}{r_m[M]+[A]} \qquad 2.1$$

[A] and [M] represent the concentrations of A and M at time t, d[A] and d[M] the amounts of A and M consumed during the time interval (t,t+dt), and $r_a = k_{aa}/k_{am}$ where k_{aa} and k_{am} are the rate constants of the respective addition of A and M to the radical A.

The molar macromonomer concentration [M] is low in relation to the molar concentration [A] in most copolymerisation experiments. Therefore, the above equation can be reduced to Jaacks' equation[14,57,58]:

$$\frac{d[A]}{d[M]} = r_a \frac{[A]}{[M]} \qquad \text{if } [A] >> [M] \qquad 2.2$$

This can be integrated to[59]:

$$r_a = \frac{\ln [A]_0/[A]}{\ln [M]_0/[M]} = \frac{\ln(1-x_a)}{\ln(1-x_m)} \qquad 2.3$$

In this equation x_a and x_m are the fractional conversions of A and M at the time t and $[A]_0$ and $[M]_0$ are the initial molar concentration of A and M in the reaction medium. From

these equations it is clear that the actual value of r_m is of no importance to the process if the molar amount of the macromonomer used in the reaction is small. The ratio of the molar amounts of A and M incorporated into the copolymer immediately is proportional to the ratio of their molar ratios in the feed of macromonomer copolymerisation. When $r_a > 1$, monomer A is consumed at a faster rate than macromonomer M, and therefore the proportion of M in the feed increases as conversion increases. This results in a higher incorporation of grafts into the copolymer. The opposite is true when $r_a < 1$. In this case macromonomer M is consumed at a higher rate than monomer A, which leads to a decrease in the percentual amount of M in the feed as conversion increases. The possibility to find an AA diad at any place along the chain can be expressed by the following equation:

$$P_{aa} = F_a \cdot \frac{k_{aa}[A]}{k_{aa}[A] + k_{am}[M]} = F_a \cdot \frac{r_a f_a}{r_a f_a + f_m} = F_a \cdot F_m \qquad 2.4$$

In this case f_a and f_m are the molar proportions of A and M in the monomer mixture, and F_a represents the mole percentage of A units in the copolymer that is formed at that instance. In a similar way, the probability of finding AM and MA diads along the chain is expressed as follows:

$$p_{am} = p_{ma} = F_a \frac{f_m}{r_a f_a + f_m} = F_m \quad \frac{r_a f_a}{r_a f_a + f_m} = F_a \cdot F_m \qquad 2.5$$

If f_m remains below 0.05, the probability of finding MM diads at any given place along the chain is negligible:

$$p_{mm} = F^2_m = \frac{f_m^2}{(r_a f_a + f_m)2} \approx 0 \qquad 2.6$$

If the molar amount of the macromonomer in the reaction mixture is small enough, these expressions lead to the conclusion that the distribution of the M units along the backbone that is formed instantaneously follows the Bernouillian statistics. Fluctuations

in composition and hereby the content of grafts in a graft copolymer sample, remains within narrow limits, provided that the conversion is not too high[60].

2.6 Anionic polymerisation for PDMS

Anionic polymerisation involves the polymerisation of a number of monomers which proceeds by the addition of the monomers to active centers, bearing a whole or partial negative charge. The active center is regenerated in each step[60]. The negatively charged chain end is often associated with an alkali metal or alkaline earth metal cation. Two main classes of monomers are susceptible to anionic polymerisations; vinyl or diene monomers and cyclic monomers. Of the cyclic monomers, ethylene oxide was probably the first monomer to be polymerised in 1878[61]. Cyclic sulphides, lactones, lactams and cyclosiloxanes can also be polymerised anionically. This study focused on the anionic polymerisation of hexamethylcyclotrisiloxane (D_3). These cylic monomers are polymerised by quite weak bases. The lithium alkyl-initiated polymerisation of D_3 is a useful method for the preparation of polydimethylsiloxane. Initiator and monomers react in hydrocarbon solvents in the following manner[62,63]:

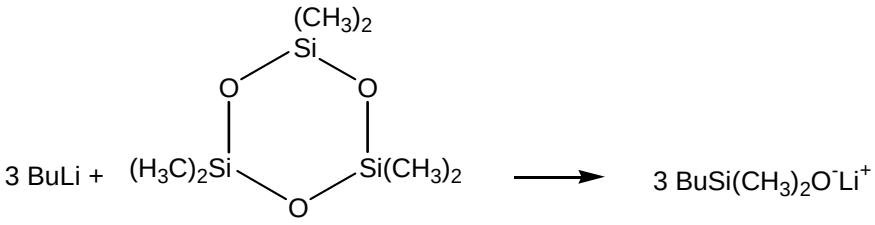

Scheme 2.1: D_3 monomer reacting with initiator during lithium alkyl-initiated polymerisation of D_3.

Chain propagation will only occur if a donor solvent such as tetrahydrofuran is added. The initiation and propagation steps are separated; propagation is fast enough that ring-chain equilibrium does not disturb the molecular-weight distribution. Anionic polymerisations are characterised by the long lifetime of the carbanionic sites[20,21] or in the case of D_3 monomers, the oxyanion site. When neither transfer nor termination reactions occur, the polymers show a narrow molecular weight distribution or polydispersity, provided initiation is fast compared to propagation.

2.7 PMMA-graft-PDMS copolymers

With PMMA-graft-PDMS copolymers, microphase-separated PDMS domains are incorporated into a PMMA matrix. This phenomenon is due to the severe incompatibility of the component polymers. Therefore this system shows many of the desirable properties of both components. PMMA is a hard glassy material with a high transition temperature[3]. It is clear due to its amorphous nature and can be used as a replacement for window glass. PDMS has a much lower glass transition temperature (Tg) and this leads to phase separation in the final copolymer. PDMS has received much attention in recent years to replace porcelain and glass insulators in high voltage applications. It has many desirable properties to make it suitable for such applications, such as elastomeric behavior, good thermal, UV and oxidative stabilities; good weatherability and electrical properties[4].

Smith *et al*.[3] analysed PMMA-g-PDMS copolymers with varying molecular weight and graft inclusion. The methacryloxy functionalised PDMS macromonomers were produced via anionic polymerisation, making it possible to control and produce macromonomers with varying molar mass. PDMS macromonomer inclusions were also varied during the free-radical copolymerisation of the PDMS macromonomers with methylmethacrylate (MMA). Transmission electron microscopy (TEM) indicated the phase separation. The domain changed from being spherical at 16 wt % PDMS, but when over 45 wt % PDMS the morphology changed to an ordered cylindrical texture. The air/solid interface is expected to be dominated by PDMS due to its low surface energy[64]. Contact angle measurements also showed that the greater the molecular weight of the PDMS macromonomers, the thicker and more complete the PDMS surface layer.

PMMA-graft-PDMS copolymer samples were separated according to chemical composition by reversed-phase high-performance liquid chromatography by Kawai and co-workers[65]. Shinoda *et al.*[66] evaluated the effect of molecular structure on morphology and mechanical properties of PMMA-graft-PDMS copolymers synthesised via controlled radical polymerisation. Compositional distribution characterisation of PMMA-graft-PDMS copolymers were done combining gradient elution high performance liquid chromatography (HPLC) and size exclusion chromatography (SEC) separation by Schunk *et al*[67]. Results indicated a relatively constant incorporation of the number of

PDMS side chains with increasing PMMA backbone molecular mass, leading to a relative decrease in weight fraction PDMS incorporation with increasing molecular mass of the whole graft copolymer.

2.8 Chromatography of polymers

2.8.1 Gradient elution chromatography

This technique is widely employed to separate polymers according to chemical composition. A simplified scenario will be shown to illustrate the use of this technique when analysing a polymer sample that contains a block copolymer (A-B), as well as small amounts of the constituent homopolymer molecules (A) and (B). These different molecules will react differently in solutions according to their solubilities. They will also interact differently with the stationary phase of the column depending on the respective polarity of the molecule and the stationary phase. Analysis can be performed in reversed phase (RP) or normal phase (NP) depending on the chromatographic system used for the particular polymer to be separated. In RP the mobile phase is polar and the stationary phase non-polar. In NP the mobile phase is non-polar and the stationary phase polar. A RP system will be used to illustrate the technique, where separation will occur due to the difference in solubilities of the different components[65]**.** The solvent used will be a mixture of (C) and (D) where (C) is a poor solvent for component (B) and (D) is a good solvent for both component (A) and (B). The solvent gradient will be started with a 100% solution of solvent C as eluent. This will cause component A to stay in solution and therefore eluting. Component B however will precipitate out due to solvent C being a poor solvent for this component and be retained on the column. The block copolymer will be partly in solution (component A) and partly precipitated (component B). As the solvent composition is gradually changed from 100% solvent C to 100% solvent D, homopolymer A will continue eluting, the block copolymer that has been in solution partly will follow and lastly homopolymer B will elute. This is illustrated in figure 2.2.

Gradients could however, be a lot more complicated, involving steps where solvent compositions are held constant for a certain period of time or complicated solvent combinations can be used in order to get separation. An example of this was illustrated

by Schunk *et al.*[67] where characterisation of poly (methyl methacrylate)-graft-polydimethylsiloxane copolymers have been done using GEC.

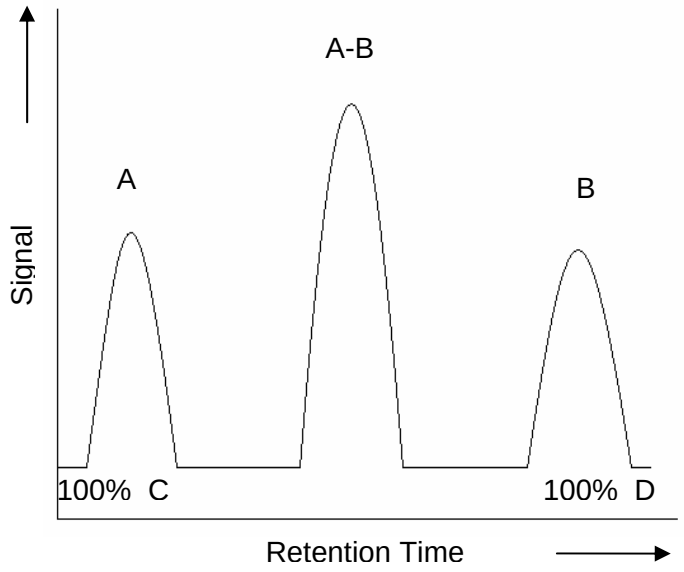

Figure 2.2: GEC elution profile of a polymer sample that contains a block copolymer and constituent homopolymer molecules.

The compositional fractionation of poly (methyl methacrylate)-graft- polydimethylsiloxane by reversed-phase GEC has been done by Kawai *et al*[65]. Graef and co-workers[68] developed GEC techniques to aid the analysis of styrene- and MMA grafted epoxidised natural rubber. Venkatesh and Klumperman[69] used GEC to prove the successful formation of block copolymer using a macroiniator technique. The behaviour of triblock copolymers with alternating sequences of segment order was compared with GEC by Park and co-workers[70].

2.8.2 Two dimensional chromatography

The growing number of heterogeneous polymers being synthesised places increasing demands on existing analytical techniques. Block or graft copolymers are complex macromolecular systems that are characterised by chemical composition distribution (CCD) and distributions in molar mass (MMD). Average molar masses and chemical compositions of copolymers can be determined by a variety of different techniques. For the determination of distribution functions, however, chromatographic separation is

required. The standard technique for MMD analysis is size exclusion chromatography (SEC), while CCD can be determined by means of interaction chromatography[71].

It has been shown that the molar masses of individual blocks in diblock and triblock copolymers can be measured by liquid chromatography at the critical point of adsorption (LCCC)[72-77]. Operating at critical conditions of one block of the copolymer, this block does not contribute to retention and behaves "chromatographically invisible" [78-80]. At the same time the other block elutes in the SEC mode and can be quantified accordingly.

To evaluate complex copolymers, a combination of different chromatographic techniques can be used. By using these techniques and combining them with each other, two-dimensional information on CCD and MMD can be obtained[81-83]. Kilz *et al*.[84-86] developed a fully automated two-dimensional chromatographic system several years ago. It consists of two chromatographs; one, a SEC instrument separates molecules by size and the other separates by chemical composition or functionality. Fractions from the first separation step are transferred into the second separation system via an online storage loop system.

A number of applications of 2D chromatography have been described, including the analysis of the grafting product of butyl acrylate onto poly(styrene-block-butadiene) by Adrian *et al*[87]. The grafting products of methyl methacrylate onto ethylene propylene diene monomer (EPDM) have been analysed in the offline mode by Augenstein and Stickler[88]. Siewing *et al*.[89] used a fully automated 2D chromatography. The characterisation of poly(alkylene oxide)s, polyesters and epoxy resins has also been described[90-93].

Graef and co-workers[68] have combined LCCC and SEC for the two-dimensional analysis of graft copolymers. Poly(styrene-block-methyl methacrylate)s were fully analysed by liquid chromatography at the critical point of adsorption (LCCC) and two-dimensional chromatography by Pasch *et al*[81]. In the first dimension, LCCC was used to separate with regard to chemical composition and in the second dimension; SEC provides information on molar mass distribution. It was shown that only when information on different chromatographic experiments is combined, a complete picture of the molecular

heterogeneity of block copolymers can be obtained. SEC alone is not appropriate for full analysis of molecular heterogeneity of such samples.

2.9 Atomic force microscopy

The atomic force microscope (AFM) is a member of the family of scanning probe microscopes (SPM). The forces acting between the sample and the probe are measured in the operating mode of all SPM's[94]. An atomically sharp probe is scanned across the sample surface, to sense interactions in the near field of the surface. These interaction forces are measured on the raster pattern for every point, which results in a three-dimensional topographical image. Besides imaging, the AFM can be used to probe physical properties locally, at specific points on the sample surface and an adhesion image is recorded. The instrument can be operated in different modes. In contact mode, the probe is so close to the sample that the interaction forces between the atoms of the sample and tip of the electrode are repulsive. This mode is preferably used on hard surfaces, where the sample surface will not be indented too much. In non-contact mode, the distance between the sample and probe is larger; therefore the interactive forces are attractive van der Waals forces. This mode is preferred for softer samples, where the contact mode might damage the sample surface. In the third intermittent contact or tapping mode, the tip touches the surface only briefly during each cycle and no lateral forces is present. This digital pulsed force mode[95] combines both techniques and generates a topographical image simultaneously with an adhesion image of the scanned area. This mode was used by Sato *et al*.[96] to determine the distribution of observed values of the adhesive forces on self-assembled sample surfaces. Okabe *et al*.[97] used chemically modified tips to discriminate the functional groups of self-assembled sample surfaces.

The AFM can be used to probe physical properties at specific points on the sample surface besides imaging. The most common method is to record a force-distance curve[98,99]. The deflection signal obtained by the distortion of the laser beam is plotted as a function of the vertical distance as the probe is lowered onto the surface and is retracted again. This is shown in figure 2.3. The cantilever is lowered from a certain height above the sample surface until it touches the surface (A to B). The cantilever is not distorted and there is no force acting on the probe in this region. The probe jumps in

contact with the surface at B and from here, the probe is in contact with the surface and the cantilever is bent upwards (B to C). For harder samples, the gradient would be greater for this part. The probe will stay in contact with the surface because it is retracted, due to the adhesive force acting between the sample and the probe (C to D). At D the cantilever is no longer distorted and comes loose from the sample surface. The force acting between the probe and the sample is measured as the distance from point D to the base line (E). The adhesive force can be calculated by multiplying the spring constant of the cantilever by the deflection E.

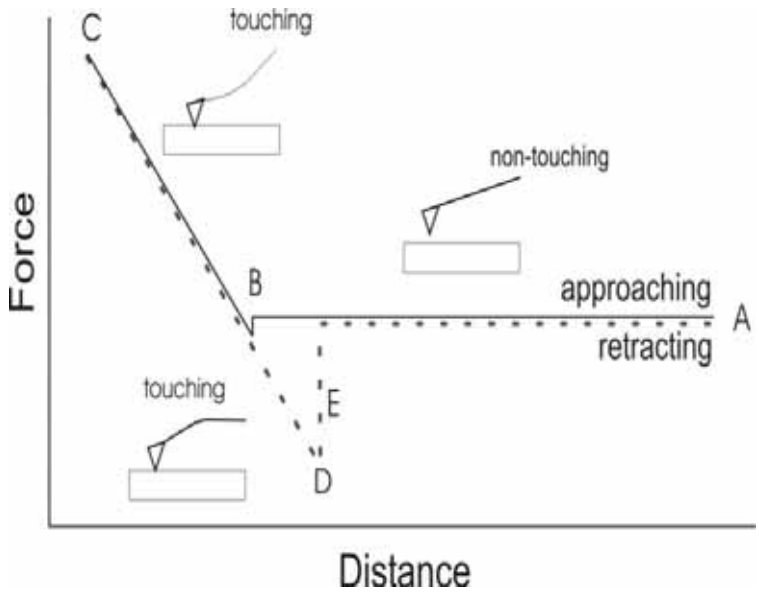

Figure 2.3: Force-distance relationship of the cantilever deflection and the vertical distance.

Work by Meincken *et al*.[94] showed the characterisation of polymers. This technique was used to show the different stages of latex film formation as well as the imaging of physical properties of polymers. The digital pulsed force mode was used for the determination of the hydrophilic character of membranes by Meincken *et al*[95].

2.10 Hydrophobic loss and recovery of PDMS

PDMS is known to show a very hydrophobic character. This very high hydrophobicity can be the result of two different phenomena[100]:

1. The methyl groups give a hydrophobic character to the polymer.
2. The silicone polymer chain is very flexible. This can result in the rearrangement of the methyl groups in order to be orientated at an interface. This nature of the silicones allows them to reorient from the bulk to the surface, presenting a layer of hydrophobic methyl groups at the surface. The large bond angle of the Si-O-Si linkage in the siloxane backbone (135 – 180°), with a minimum energy at 145°, leads to the high chain flexibility and makes it easy for the methyl groups to reorient from the bulk to the surface.

A hydrophobic surface is defined as a surface which is not readily wettable. 'Water hating' or hydrophobic materials have no or very little tendency to adsorb water and water forms discrete droplets (beads) on their surfaces. Hydrophobic materials lack active groups in their surface chemistry for the formation of hydrogen bonds with water and possess a very low surface tension. The intermolecular attraction that causes surface tension is due to a variety of intermolecular forces. Most of these forces, such as hydrogen bonding forces or London dispersion forces are functions of the chemical nature. London dispersions results in an attractive force between adjacent atoms or molecules and exists in all matter. In the case of PDMS, the hydrogen bonding force is smaller than the London dispersion force and this gives PDMS its hydrophobic character[101].

It is well known that PDMS loses this hydrophobic property when exposed to corona discharges in air by oxidation. Many researchers have employed corona and oxygen plasma to treat and investigate the loss and recovery of hydrophobicity of silicone rubber over the last 35 years[102]. Another factor that can also lead to the loss of hydrophobicity is long-term submersion in water. This could be due to the hydrolysis of the siloxane bonds and the creation of hydrophilic end groups at the surface[103,104]. The increase in the average oxygen content bonded to the silicone atom is due to the highly oxidised surface layers. A crosslinked, brittle silica-like structure may also form. Polar hydroxyl

groups are also formed. Both these factors lead to an increase in the hydrophilicity of the surface[103,105,106].

It has been suggested that oxidation results in the formation of in inorganic silica-like (SiO_x) structure – a silicone atom bonded to more than two oxygen atoms, which lead to an increase in the hydrophilicity of the surface. However, silicone elastomers have the unique characteristic to readily recover their original hydrophobicity if enough time is given.

This change from a hydrophilic to a hydrophobic surface is referred to as hydrophobicity recovery. This recovery can be explained as being due to one of the following mechanisms[107]:

1. Condensation of the surface hydroxyl groups.
2. *In situ* created LMW (low molecular weight) species migrate to the surface during discharge.
3. Pre-existing LMW silicone fluid diffuse from the bulk to the surface.
4. Polar groups reorient from the surface to the bulk phase or the non-polar groups reorient from the bulk to the surface.

A number of researchers have suggested in literature that the main mechanisms for the long term stability of hydrophobicity recovery in the case of PDMS are surface reorientation and diffusion of LMW species[108]. On the other hand, Morra *et al.*[109] suggested that the burial of the polar groups into the bulk accompanied by the condensation of the surface silanol and crosslinking in the contact angle probed layer leads to the hydrophobic recovery. Several mechanisms have been proposed to account for the recovery, but many agree that migration of the low molar mass PDMS oligomers to the surface is the dominant mechanism [110-112].

Mallon *et al.*[104] studied a phenomenon involving corona treatment. It was shown that after corona treatment, an ultra thin silica layer formed at the surface of the material. All characteristic hydrophobicity of the material was lost upon treatment, but the hydrophobicity was regained when the material was left untreated. Properties like this make it extremely interesting to see how this polymer would behave if grafted onto a firmer and more glassy material like PMMA.

2.11 Positron annihilation spectroscopy

Positron annihilation spectroscopy (PAS)[113] has been developed as one of the most successful techniques for the direct examination of local free volume holes in polymers. A number of techniques have been used to evaluate the free volume properties of polymers. Transmission electron spectroscopy (TEM) and scanning electron microscopy (SEM) are sensitive to static holes that have a size of 10 Å or larger. Scanning tunneling microscopy (STM) and atomic force microscopy (AFM) are probing techniques used to prove defects in materials and are sensitive to angstrom size holes. The use of these techniques is limited in polymers, since the techniques are limited to static holes on the surface. Small angle x-ray scattering and neutron diffraction can be used to determine density fluctuations and deduce free volume size distributions. Figure 2.4 shows a comparison of these probing techniques in terms of their ability to resolve defect size and concentration.

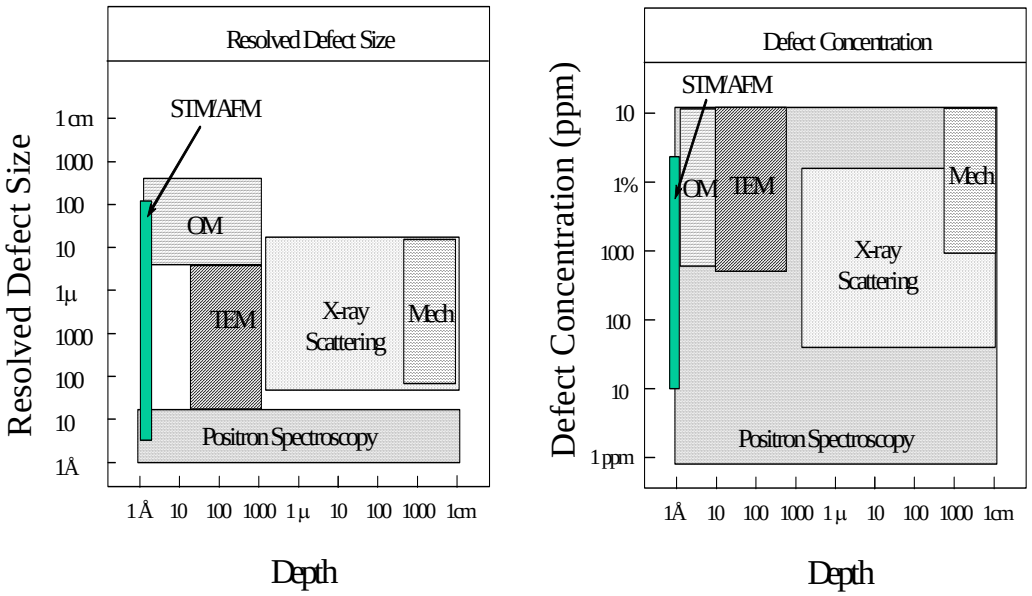

Figure 2.4: Comparision of various techniques for examination of defects and voids in materials (OM-optical microscopy, TEM- transmission electron microscopy, STM-Scanning tunneling microscopy, AFM-atomic force microscopy and Mech-mechanical techniques).

PAS are particularly sensitive due to the small size of the positronium probe (1.59 Å). The o-Ps has a relatively short lifetime and therefore PAL can probe holes due to molecular motion from 10^{-10} s or longer. Unlike other methods, PAL can determine the

local hole size and free volume in a polymer without being interfered with by the bulk significantly. PAL does not only give information on the free volume size and fractions of free volume, but also gives detailed information on the distribution of free volume hole sizes.

Positrons (e^+) are the anti-particles of electrons (e^-). They are produced in a radioactive source such as Germanium-68. The bonded state of an electron and a positron is a positronium (Ps). There are two states in which positroniums can be formed: ortho-positroniums (spins aligned) and para-positroniums (spins anti-aligned). Positron techniques are based on the measurement of the annihilation radiation produced when positrons implanted into the polymer matrix and electrons in the polymer matrix meet and annihilate. Both the positron and electron are destroyed in the annihilation process and their masses are converted to energy. Since a positron is basically the anti-matter of an electron, this annihilation process can occur.

The basic principle of PAS lies in the fact that the electromagnetic interaction between the electrons and positrons make their annihilation possible. The total energy of the e^+-e^- pair may be transferred to photons. These annihilation gamma photons carry information on the electronic environment in which the positron annihilates. Crystal point defects attract these positrons and therefore the electronic environment sensed, is often that of defect in the sample under investigation. Due to the localization of the positronium in the free volume holes of polymers, positron annihilation techniques are the most sensitive techniques for tracking changes that occur in the polymer structure. By this technique information can be obtained about defect size, concentration and location of the free volume holes in most solid materials.

Doppler broadening of energy spectra (DBES) and positron annihilation lifetime measurements (PAL) are the two main types of positron experiments in polymers using a positron beam. The DBES spectra is characterised by an S parameter, which is defined as the ratio of integrated counts in the central part of the peak to the total counts after the background is subtracted. In DBES, only the p-Ps part of the PS annihilation contributes to the S parameter. Three main factors contribute to the S parameter in polymers for DBES data: (1) free volume size, (2) free-volume content and (3) chemical composition. Therefore, a larger free-volume contributes to a larger S value. In a

polymer with defects or voids, the S parameter is a qualitative measure of the defect concentration and size. The S parameter also depends on the electron momentum of the elements, as well as the momentum of the valence electrons, which annihilate with the positrons. This means that the absolute value of the S parameter may vary from polymer to polymer. The S parameter may vary according to the chemical nature of the polymer.

The S-parameter decrease significantly upon ageing of polymers due to weathering. Slow-positron beam techniques are very successful in monitoring these changes. One of the great values of this technique is the depth-profiling ability, which allows for the determination of kinetic data of the degradation process as a function of the depth from the surface.

When a positron with a well-defined energy is accelerated from a vacuum into a polymer, it either reflects back to the surface or penetrates into the polymer. The fraction of positrons that enter the polymers increases rapidly as a function of positron energy. As the positrons enter the polymer, the positrons are slowed down by inelastic collisions between the positron and molecules. The mean implementation depth as a result of inelastic interactions with polymer molecules is expressed as[114]:

$$Z(E_+) = [(40 \times 10^3)/\rho] E_+^{1.6} \qquad 2.7$$

Where Z is the thickness in nanometers, ρ is the density in kilograms per cubic meter and E_+ is the incident energy in kiloelectronvolts. Depth profiling information on the free volume properties of the polymer can therefore be obtained by controlling the implantation energy.

Mallon *et al.*[5] has recently shown that this technique provides unique information on material changes in PDMS based compounds that are used in high voltage insulators when these compounds are treated with corona. Evidence was found in the S-parameter depth profiles for the formation of a silica-like layer on corona treatment of samples. The S-parameter increases at very low positron implantation energies and reaches a maximum plateau followed by a decrease in samples with formulations similar to those used commercially. This profile was attributed to the effects of the alumina trihydrate (ATH) filler.

Mallon *et al*.[104] has also showed that there are large changes in the S parameter profiles of pure PDMS compounds used in outdoor high voltage insulators as a function of the positron implantation depth when they are exposed to various corona treatment times. The S parameter profiles can be explained by the formation of a silica-like layer of about 40nm at the surface of the polymer due to degradation of the polymer. Useful information on the mechanisms of degradation and the formation of a silica-like layer in these compounds can be provided by positron beam techniques.

2.12 References

(1) Pyun, J.; Matyjaszewski, K. *Chem. Mater.* **2001**, *13*, 3436-3448.

(2) Shinoda, H.; Miller, P. J.; Matyjaszewski, K. *Macromolecules* **2001**, *34*, 3186-3194.

(3) Smith, S. D.; DeSimone, J. M.; Huang, H.; York, G.; Dwight, D. W.; Wilkes, G. L.; McGrath, J. E. *Macromolecules* **1991**, *25*, 2575-2581.

(4) Lee, Y.; Akiba, I.; Akiyama, S. *J. Appl. Polym. Sci.* **2003**, *87*, 375-380.

(5) Mallon, P. E.; Greyling, C. J.; Vosloo, W.; Jean, Y. C. *Radiat. Phys. Chem.* **2003**, *68*, 453-456.

(6) Itsuno, S.; Uchikoshi, K.; Ito, K. *J. Am. Chem. Soc.* **1990**, *112*, 8187.

(7) Hong, K.; Uhrig, D.; Mays, J. W. *Curr. Opin. Solid State Mater. Sci.* **1999**, *4*, 531-538.

(8) Rahlwes, D.; Roovers, J. E. L.; Bywater, S. *Macromolecules* **1977**, *10*, 604.

(9) Allen, G.; Eastmond, G. C.; Ledwith, A.; Russo, S.; Sigwalt, P. *Comprehensive Polymer Science*, *6*, 403-419.

(10) Se, K.; Watanabe, O.; Shibamoto, T.; Fujimoto, T. *Polym. Prepr.* **1988**, *29*, 110.

(11) Inoki, M.; Akutsu, F.; Yamaguchi, H.; Naruchi, K.; Miura, M. *Macromol. Chem. Phys.* **1994**, *195*, 2799.

(12) Jannasch, P.; Wesslen, B. *J. Polym. Sci., Part A: Polym. Chem.* **1995**, *33*, 1465.

(13) Bhattacharya, A.; Misra, B. N. *Prog. Polym. Sci.* **2004**, *29*, 767-814.

(14) Milkovitch, R.; Chiang, M. T. *Polym. Prepr. (Am. Chem. Soc.,Div. Polym. Chem.)* **1974**, *21*, 40.

(15) Rempp, P. F.; Strazielle, C.; Lutz, P. *Encyclopedia of Polymer Science*, *9*, 195-203.

(16) Ito, K. *Prog. Polym. Sci.* **1998**, *23*, 581-620.

(17) Rempp, P. F.; Franta, E. *Adv. Polym. Sci.* **1984**, *58*, 1-53.

(18) Greber, G.; Balciunas, A. *Makromol. Chem.* **1963**, *69*, 193.

(19) Chaumont, P.; Herz, J.; Rempp, P. F. *Eur. Polym. J.* **1979**, *15*, 537.

(20) Quirk, R. P. *Comprehensive Polymer Science* **1992**, *1st Suppl. Pergamom Press, Oxford*, 83.

(21) Hirao, A.; Nakahama, S. *Prog. Polym. Sci.* **1992**, *17*, 283.

(22) Milkovitch, R. *ACS Symp. Ser.* **1981**, *166*, 41.

(23) Schulz, G. O.; Milkovitch, R. *J. Appl. Polym. Sci.* **1982**, *27*, 4773.

(24) Rempp, P.; Loucheux, M. H. *Bull. Soc. Chim. Fr.* **1958**, 1497.

(25) Asami, R. *IUPAC 28th Symp. On Macromolecules* **1982**, 71.

(26) Lutz, P.; Masson, P.; Beinert, G.; Rempp, P. *Polym. Bull.* **1984**, *12*, 79-85.

(27) Quirk, R. P.; Yoo, T. *Polym. Bull.* **1993**, *31*, 29-36.

(28) Ishizu, K.; Furukawa, T. *Polymer* **2001**, *42*, 7233-7236.

(29) Sawamoto, M. *Prog. Polym. Sci.* **1991**, *16*, 111.

(30) Dreyfuss, P.; Dreyfuss, M. P. *Adv. Polym. Sci.* **1967**, *4*, 528.

(31) Penczek, S.; Kubisa, P.; Matyjaszewski, K. *Adv. Polym. Sci.* **1980**, *37*.

(32) Kennedy, J. P. *Polym. J.* **1980**, *12*, 609.

(33) Kennedy, J. P.; Smith, R. A. *Polym. Prepr. (Am. Chem. Soc.,Div. Polym. Chem.)* **1979**, *20*, 316.

(34) Chang, V.; Kennedy, J. P. *Polym. Bull.* **1981**, *5*, 379.

(35) Ivan, B.; Kennedy, J. P.; Chang, V. *J. Polym. Sci.* **1980**, *18*, 1523.

(36) Kennedy, J. P.; Liao, J. P. *Polym. Bull.* **1981**, *5*, 11.

(37) Percec, V. *Polym. Bull.* **1982**, *8*, 25.

(38) Flory, P. J. *Principles of Polymer Chemistry* **1953**, *Cornell University Press, Ithaca, N.Y.*

(39) Odian, G. *Principles of Polymerization* **1991**, *3rd edn. Wiley, New York*.

(40) Nguyen, H. A.; Marechal, E. *J. Macromol. Sci.* **1988**, *C28*, 187.

(41) Otsu, T.; Matsunaga, T.; Doi, T.; Matsumoto, T. *Eur. Polym. J.* **1995**, *31*, 67.

(42) Kazmeier, P. M.; Moffat, K. A.; Georges, M. K.; Veregin, R. P. N.; Hamer, G. M. *Macromolecules* **1995**, *28*, 1841.

(43) Hawker, C. J.; Hedrick, J. L. *Macromolecules* **1995**, *28*, 2993.

(44) Wang, J.; Matyjaszewski, K. *J. Am. Chem. Soc.* **1995**, *117*, 5614.

(45) Mardare, D.; Matyjaszewski, K. *Macromolecules* **1994**, *27*, 645.

(46) Kato, M.; Kamigaito, M.; Sawamoto, M.; Higashimura, T. *Macromolecules* **1995**, *28*, 1721.

(47) Konter, W. *Makromol. Chem.* **1981**, *182*, 2619.

(48) Moad, G.; Solomon, D. H. *The Chemistry of Radical Polymerisation*: Heidelberg: Elsevier, 2006.

(49) Asher, M.; Vofsi, D. *J. Chem. Soc. (B)* **1963**, 1887.

(50) Boutevin, B.; Pietrasanta, Y. *J. Polym. Sci.* **1981**, *19*, 499.

(51) Boutevin, B.; Pietrasanta, Y.; Taha, M. *Makromol. Chem.* **1982**, *183*, 2977.

(52) Boutevin, B.; Pietrasanta, Y.; Sideris, A. *J. Fluorine Chem.* **1982**, *20*, 727.

(53) Ito, K. In *Chemistry and Industry of Macromonomers*; Yamashita, Y.; Huthig; Verlag, W., Eds.: Basel, 1993.

(54) Tsukahara, Y. In *Chemistry and Industry of Macromonomers*; Yamashita, Y.; Huhtig; Verlag, W., Eds.: Basel, 1993.

(55) Meijs, G. F.; Rizzard, E. *J. Macromol. Sci. Rev.* **1990**, *C30*, 305.

(56) Kawakami, Y. *Prog. Polym. Sci.* **1994**, *19*, 203.

(57) Vargas, J. S.; Franta, E.; Rempp, P. F. *Makromol. Chem.* **1981**, *182*, 2063.

(58) Jaacks, V. *Makromol. Chem.* **1972**, *161*, 161.

(59) Kennedy, J. P.; Lo, C. Y. *Polym. Bull.* **1982**, *8*, 63.

(60) *Encyclopedia of Polymer Science*, *2*, 1-11.

(61) Wurz, A. *C.R.* **1978**, *86*, 1176.

(62) Lee, C. L.; Frye, C. L.; Johannson, O. K. *Polym. Prepr. (Am. Chem. Soc.,Div. Polym. Chem.)* **1969**, *10*, 1361.

(63) Morton, A. A.; Bolton, F. H.; Collins, F. W.; Cluff, E. F. *Ind. Eng. Chem.* **1952**, *44*, 2876.

(64) Hillborg, H.; Sandelin, M.; Gedde, U. W. *Polymer* **2001**, *42*, 7349-7362.

(65) Kawai, T.; Akashima, M.; Teramachi, S. *Polymer* **1995**, *36*, 2851-2852.

(66) Shinoda, H.; Matyjaszewski, K. *Macromolecules* **2003**, *36*, 4772-4778.

(67) Schunk, T. C.; Long, T. E. *J. Chromatogr. A* **1995**, *692*, 221-232.

(68) Graef, S. M.; Van Zyl, A. J. P.; Sanderson, R. D.; Klumperman, B.; Pasch, H. *J. Appl. Polym. Sci.* **2003**, *88*, 2530-2538.

(69) Venkatesh, R.; Klumperman, B. *Macromolecules* **2004**, *37*, 1226-1233.

(70) Park, I.; Park, S.; Cho, D.; Chang, T.; Kim, E.; Lee, K.; Kim, Y. J. *Macromolecules* **2003**, *36*, 8539-8543.

(71) Pasch, H. In *Chapters 1,2 and 3. HPLC of Polymers*; Pasch, H.; Trathnigg, B., Eds.; Springer-Verlag: Berlin, 1998.

(72) Pasch, H.; Much, H.; Schulz, G.; Gorshkov, A. V. *LC-GC Internat.* **1992**, *5*, 38.

(73) Gankina, E.; Belenkii, B.; Malakhova, I. *J. Planar Chromatogr.* **1991**, *4*, 191.

(74) Zimina, T. M.; Kever, J. J.; Melenevskaya, E. Y.; Fell, A. F. *J. Chromatogr.* **1992**, *593*, 233.

(75) Pasch, H.; Brinkmann, C.; Gallot, Y. *Polymer* **1993**, *34*, 4100.

(76) Pasch, H.; Gallot, Y.; Trathnigg, B. *Polymer* **1993**, *34*, 4986.

(77) Pasch, H.; Brinkmann, C.; Much, H.; Just, U. *J. Chromatogr.* **1992**, *623*, 315.

(78) Gorbunov, A. A.; Skvortsov, A. M. *Vysokomol. Soedin. (A)* **1988**, *30*, 453.

(79) Gorbunov, A. A.; Skvortsov, A. M. *Vysokomol. Soedin. (A)* **1988**, *30*, 895.

(80) Entelis, S. G.; Evreinov, V. V.; Gorshkov, A. V. *Adv. Polym. Sci.* **1986**, *76*, 129.

(81) Pasch, H.; Trathnigg, B. *HPLC of polymers*; Springer: Berlin-Heidelberg-New York, 1998.

(82) Pasch, H. *Adv. Polym. Sci.* **1997**, *128*, 1.

(83) Pasch, H. *Adv. Polym. Sci.* **2000**, *150*, 1.

(84) Kilz, P. *Labor Praxis* **1993**, *6*, 64.

(85) Kilz, P.; Kruger, R. P.; Much, H.; Schulz, G. *ACS Adv. Chem.* **1995**, *247*, 223.

(86) Kilz, P.; Kruger, R. P.; Much, H.; Schulz, G. *PMSE Prepr.* **1993**, *69*, 114.

(87) Adrian, J.; Esser, E.; Hellmann, G.; Pasch, H. *Polymer* **2000**, *41*, 2439.

(88) Augenstein, M.; Stickler, M. *Makromol. Chem.* **1990**, *191*, 415.

(89) Siewing, A.; Schierholz, J.; Braun, D.; Hellmann, G.; Pasch, H. *Macromol. Chem. Phys.* **2001**, *202*, 2890.

(90) Trathnigg, B.; Maier, B.; Yan, X. *Proc. 7th Int. Symp. Polym. Anal. Char.* **1994**.

(91) Adrian, J.; Braun, D.; Pasch, H. *LC-GC Internat.* **1998**, *11*, 32.

(92) Kruger, R. P.; Much, H.; Schulz, G. *Int. J. Polym. Anal. Char.* **1996**, *2*, 221.

(93) Adrian, J.; Braun, D.; Pasch, H. *Angew. Makromol. Chem.* **1999**, *267*, 82.

(94) Meincken, M.; Sanderson, R. D. *S. Afr. J. Sci.* **2004**, *100*, 256-260.

(95) Meincken, M.; Roux, S. P.; Jacobs, E. P. *Appl. Surf. Sci.* **2005**, *252*, 1772-1779.

(96) Sato, F.; Okui, H.; Akiba, U.; Suga, K.; Fujihira, M. *Ultramicroscopy* **2003**, *97*, 303-314.

(97) Okabe, Y.; Akba, U.; Fujihira, M. *Appl. Surf. Sci.* **2000**, *157*, 398-404.

(98) Weisenhorn, A.; Maivald, P.; Butt, H.; Hansma, P. *Phys. Rev. B* **1992**, *45*, 11226-11232.

(99) Sheiko, S. *Adv. Polym. Sci.* **2000**, *151*, 61-174.

(100) Brook, M. A. **2000**.

(101) Kim, S. H.; Cherney, E. A.; Hackam, R. *IEEE . Trans. Diel. Elect. Insul.* **1992**, *27*, 610-612.

(102) J.R., H.; Carlson, G. L. **1970**, *14*, 2499-2508.

(103) Hackam, R. *IEEE Trans. Diel. Elect. Insul.* **1999**, *6*, 556-585.

(104) Mallon, P. E.; Berhane, T. A.; Greyling, C. J.; Vosloo, W. L.; Chen, H.; Jean, Y. C. *Mater. Sci. Forum* **2004**, *445-446*, 322-324.

(105) Hillborg, H.; Gedde, U. W. *Polymer* **1998**, 1991-1998.

(106) Yoshimura, S.; Kumgai, S.; Nishimura, S. *IEEE Trans. Diel. Elect. Insul.* **1999**, *6*, 632-649.

(107) Kim, J.; Chaudhury, M. K.; Owen, M. J.; Orbeck, T. *J. Colloid Interface Sci.* **2001**, 200-207.

(108) Toth, A.; Bertoti, I.; Biazso, M.; Banhegyi, G.; Bognar, A.; Szapionczay, P. *J. Appl. Polym. Sci.* **1994**, *52*, 1293-1307.

(109) Morra, M.; Occhiello, E.; Marola, R.; Garbassi, F.; Humphrey, P.; Johnson, D. *J. Colloid Interface Sci.* **1990**, *137*, 11-24.

(110) Kim, S. H.; Cherney, E. A.; Hackam, R.; Rutherford, K. G. *IEEE . Trans. Diel. Elect. Insul.* **1994**, *1*, 106-122.

(111) Janssen, H.; A., H.; Karner, H. C. *The loss and recovery of hydrophobicity on silicone rubber surfaces, 10th inter. symp. on high voltage engi. Montreal Canada* **1997**.

(112) Gorur, R. S.; Chang, J. W.; Amburgey, O. G. *IEEE. Trans. Power Deli* **1990**, *5*, 1923-1928.

(113) Jean, Y. C.; Mallon, P. E.; Zhang, R.; Chen, H.; Wu, Y.; Li, Y.; Zhang, J. In *Chapter 11: Applications of Slow Positrons to Polymeric Surfaces and Coatings. Principles and Applications of Positron and Positronium Chemistry.*; Jean, Y. C.; Mallon, P. E.; Schrader, D. M., Eds.; World Scientific Publishing: Singapore, 2003.

(114) Cao, H.; Zhang, R.; Sundar, C. S.; Yuan, J. P.; He, Y.; Sandreczki, C.; Jean, Y. C. *Macromolecules* **1998**, *31*, 6627-6635.

Chapter 3

Experimental

3.1 Materials

Solvents toluene (Kimix, 99.8%) and tetrahydrofuran (THF, R&S enterprises, 99.0%) were dried and distilled over sodium metal and benzophenone (BP, Sigma, 98%) under argon (Ar, Afrox Scientific UHP Cyl 17.4kg N5.0, 99.999%) prior to use. Hexane (Aldrich) was washed with concentrated sulphuric acid (H_2SO_4), a concentrated solution of potassium permanganate ($KMNO_4$), a concentrated sodium carbonate solution (Na_2CO_3) and lastly with distilled water. The solvent was dried over anhydrous calcium chloride ($CaCl_2$) and distilled. Methylmethacrylate monomer (MMA, Plascon, tech. grade) was washed with a 0.3M potassium hydroxide (KOH, Associated Chemical Enterprises, 85%) solution and water. It was dried over excess magnesium sulphate ($MgSO_4$, Riedel-de Haen, 99.5%) overnight, distilled and stored at 0 ˚C prior to use. Triethylamine (Et_3N, Aldrich,99.5%), hexamethylcyclotrisiloxane (D_3, Aldrich, 98%); chlorodimethylsilane (CDMS,Aldrich, 98%); Butyllithium (BuLi, Aldrich,15% in hexane); [3-(methacryloxy)propyl]-dimethylchlorosilane (MPDC, Aldrich, 98%) and poly(dimethylsiloxane), monomethacryloxypropyl terminated (MMP-PDMS,Gelest Inc., Mw: 1000; 5000; 10000) were used as received. Grafting reactions were performed under nitrogen (N_2, Afrox Scientific UHP Cyl 11 kg N5, 99.999%) with 2,2'-azobis(isobutyronitrile) (AIBN) as initiator. Methanol (MeOH, Sasol, Class 3) was used to precipitate out the synthesised graft copolymer. Solvents for chromatography analysis were tetrahydrofuran (THF, HPLC grade), cyclohexane (99.9%), ethanol (HPLC grade) and toluene (HPLC grade) all supplied by Sigma-Aldrich.

3.2 Synthesis of macromonomers

3.2.1 Purification of solvents

Toluene and THF were placed on sodium metal and benzophenone. Permanent distillation set-ups were used and solvents were used directly after being distilled.

The cleaning of the hexane involved the following: Most of the unsaturated hydrocarbons were removed by shaking three times with 10% of the volume of concentrated sulphuric acid. The next step involved vigorous shaking with a concentrated solution of potassium permanganate in 10% sulphuric acid. The colour of the permanganate remained unchanged upon the shaking. The solvent was washed twice with a concentrated sodium carbonate solution and lastly it was washed twice with water. The solvent was dried over anhydrous calcium chloride and distilled[1]. Preparation of the dichloromethane used in the reactions included drying first, by stirring over $CaCl_2$ overnight. The solvent was distilled and stored over molecular sieves.

3.2.2 Anionic synthesis of the macromonomers

Macromonomers of various lengths were synthesised by varying the monomer: initiator ratio. Anionic reactions need to be carried out under extremely dry and air-free conditions. The preparation of reagents used is of the uttermost importance to ensure results. All glassware, including syringes and reaction vessels, were rigorously cleaned and dried in an oven at 120 ˚C overnight.

Anionic polymerisations were carried out according to the method reported earlier[2,3]. Anionic polymerisations were carried out under argon in a rigorously cleaned and dried Schlenk-tube equipped with a magnetic stirrer and rubber septum. Reaction vessels were purged with argon before use and stainless steel needles and glass syringes were used to avoid contamination due to plastic dissolution. The solid monomer, hexamethylcyclotrisiloxane (D_3) was placed in the Schlenk-tube inside a glovebox under nitrogen. Calculated amounts of toluene and tetrahydrofuran (THF) were introduced into the reaction flask with a syringe. A calculated amount of n-butyllithium was added to initiate the ring-opening polymerisation. The propagation reaction was allowed to proceed by stirring the colourless reaction mixture under argon at room-temperature for 2 hours.

A calculated amount of [3-(methacryloxy)propyl]-dimethylchlorosilane (MPDC), dissolved in freshly distilled hexane was added into the reaction mixture to terminate the reaction, to afford the macromonomer. The reaction is hereby terminated with MPDC. The

heterogeneous white reaction mixture was stirred at room temperature overnight. The mixture was diluted with hexane and filtered through a 0.45 µm filter to remove all lithium chloride (LiCl) salts. The solvent was removed from the filtrate under vacuum at 60 °C for 4 hours using a rotary evaporator. The macromonomer was stored in a fridge.

The degree of polymerisation at the end of polymerisation is directly proportional to M_0/I_0, where M_0 and I_0 are the initial monomer and initiator concentrations[4].

$$DP_n = [M_0]/[I_0] \quad 3.1$$

Therefore, by varying the ratio of M_0 to I_0, the degree of polymerisation (molar mass) of the macromonomer obtained can be controlled. The ratio of M_0 to I_0 was varied in the reactions below in order to control the molar mass of the macromonomers obtained.

Table 3.1: Reactants used in various anionic polymerisation reactions.

Reaction	D_3 monomer(g)	THF(mL)	Toluene(mL)	Butyllithium (mL)	MPDC(g)
AP1	4.99	~2.00	~2.00	0.6	0.575
AP2	3.010	~1.50	~1.5	0.5	0.4100
AP3	5.000	~2.50	~2.5	0.1	0.5732
AP4	4.983	~3.75	~1.5	0.1	0.5490
AP5	4.995	~3.75	~1.5	0.1	0.5650
AP6	7.076	~5.00	~2.0	0.1	0.8200

3.3 Grafting reactions

The characteristics of the graft copolymers synthesised, were varied by changing the ratio of MMA : PDMS macromonomer as well as using macromonomers of various lengths. Macromonomers were synthesised via living anionic polymerisation[3]. In addition to the synthesised macromonomers a set of commercially available macromonomers of three different molar masses (Mn = 1000, 5000 and 10 000) were also purchased. These were also used in the grafting reactions.

Poly(methyl methacrylate)-graft-polydimethylsiloxane were synthesised according to the method reported by *Mera et al*[5].

Preparation of the materials: Toluene was distilled and stored over molecular sieves. Methylmethacrylate monomer was washed with a 0.3M KOH solution, and water. It was dried over $MgSO_4$ overnight, distilled and stored in the fridge.

The copolymerisation of the methacryloyl-terminated macromonomer and MMA was performed at 75 °C in toluene using AIBN as initiator. Different ratios of PDMS macromonomer:MMA was used, but the percentage solids was kept constant at 20%. The ratio of initiator:MMA was also kept constant. The grafting reaction was allowed to run under reflux with a constant nitrogen flow for 50 hours. The product was precipitated in methanol and the unreacted macromonomer was extracted twice with hexane. The extracted and purified product was analysed.

3.4 NMR

NMR analyses were done at the University of Stellenbosch's NMR laboratory on a Varian VXR, 300 MHz, Spectrometer and a Varian *Unity*Inova, 600 MHz NMR instrument respectively. The Varian VXR, 300MHz spectrometer was used to perform routine ^{1}H-NMR and ^{13}C-NMR analysis for the determination of molecular structure. The Varian *Unity*Inova, 600 MHz NMR instrument was used where more precise integration data were required. Samples were prepared by dissolving 20-30 mg of the sample in deuterated chloroform (*d*-chloroform).

3.5 Room temperature size exclusion chromatography

Polymer molecules are separated according to size or hydrodynamic volume by this chromatographic technique. This technique is also referred to as gel permeation chromatography (GPC).

The SEC analyses were performed on a Waters instrument consisting of the following components:

- Millennium^{32}V3.05 Software (Control, data acquisition and processing).

- Waters 717_{plus} Autosampler
- Waters 410 Differential Refractometer at 30.0 °C
- Waters 600E System Controller
- Pump: Waters 610 fluid Unit
- Waters 2414 Refractive Index (RI) detector at 30.0˚C

Column set:

- 1 PLgel 5µm guard 50x7.5mm (Polymer Laboratories)
- 2 PLgel 5µm mixed-C 300x7.5mm (Polymer Laboratories)

The stationary phase consists of a highly crosslinked porous polystyrene/divinylbenzene matrix.

- Eluent: HPLC-grade THF (0.125% BHT stabilized) sparged with IR-grade helium
- Injection volume: 100µL
- Runtime: 30 min
- Sample concentration: 5mg/mL
- Column oven @ 30°C
- Flow rate = 1mL/min

Molar mass determination is relative to narrow polystyrene standards calibration. (EasiVial PS from Polymer Laboratories).

Due to the almost identical refractive indexes of PDMS and THF, the RI detector was not suitable for obtaining chromatograms of the PDMS material.

3.6 Room temperature SEC for low molar mass polymers and homoPDMS

The SEC analyses for low molar mass polymers and homoPDMS were performed on an instrument consisting of the following components:

SEC system:

- Waters 2690 separation module Alliance
- Evaporative light scattering detector (ELSD) PL-ELS 1000 from Polymer Laboratories

Control, data acquisition and processing:

- PSS Win GPC7 (Polymer Standards Service)

Column Set:

- 1 PLgel 3µm mixed-E 300x7.5mm (Polymer Laboratories)

The stationary phase consists of a highly crosslinked porous polystyrene/divinylbenzene matrix.

- Temperature: 30°C
- Solvent: THF Chromasolve HPLC grade
- Flow rate: 1mL/min

Molar mass determination is relative to narrow polystyrene standards calibration. (EasiVial PS from Polymer Laboratories).

The RI detector can not be used in the determination of the molecular mass of homoPDMS in THF, due to the similar refractive index of THF and PDMS and instead a PL-ELS 1000 Evaporative light scattering detector (ELSD) was used.

3.7 Gradient elution chromatography

3.7.1 HPLC equipment and experimental conditions

Gradient elution chromatography (GEC) is widely employed to separate polymers according to their chemical composition. This separation of polymer molecules is achieved by varying the mobile phase solvent composition. This technique was performed on a Waters Alliance system, consisting of the following components:

- Waters 2690 Separations module (Alliance)
- Polymer Laboratories PL-ELS 1000, Evaporative light scattering detector (ELSD)
- PSS Win GPC6 for control, data collection and processing. (Polymer standards Service)
- Supelco Nucleosil silica column: 100 Å, 5µm, 250x46(ID) mm.

The evaporiser and nebuliser temperatures of the ELSD were fixed at 120°C and 90°C, respectively. A flow rate of 1mL/min was maintained throughout the analysis. The injection volume was 30µL.

3.7.2 Solvents

The solvents used for HPLC analysis were solvent B (10% ethanol in toluene) and cyclohexane supplied by Sigma-Aldrich.

3.7.3 Sample Preparation

All samples were prepared to a concentration of 5 mg/mL. Samples were dissolved in solvent B first and then the composition of the solvent was changed to 65% solvent B and 35% cyclohexane. Samples were filtered with a 0.45µm filter. Injection volumes of 30 µL were maintained for all of the samples.

3.8 Two dimensional chromatography

Complex polymers, such as graft copolymers are distributed in more than one direction of molecular heterogeneity. For the characterisation of different types of molecular heterogeneity it is necessary to use a wide range of analytical techniques. These techniques should be selective toward a specific type of heterogeneity. The combination of two selective analytical techniques is assumed to yield two dimensional information on the molecular heterogeneity.

Increasing demands are placed on existing analytical techniques by the growing number of heterogeneous polymeric species that are being synthesised. Size exclusion chromatography (SEC) is a powerful analytical tool, though it has its limits when complex polymers e.g. graft copolymers, must be analysed. SEC yields true molar masses for linear polymers, though problems could be encountered for more complex polymers such as copolymers or branched polymers.

The analysis of graft copolymers is even more complicated, because in addition to MMD, branching distributions and chemical heterogeneity are encountered. Two dimensional chromatography can be an useful complementary technique to SEC[6].

In this study separation in the first dimension was based on chemical composition. Samples were separated according to chemical composition in the first dimension using gradient elution chromatography (GEC). Fractions from the first separation step were automatically transferred to the second dimension via an online storage loop system and separation according to hydrodynamic volume (by SEC) took place in the second dimension.

3.8.1 Two dimensional chromatography equipment and experimental conditions

Equipment:

- A modular chromatographic system consisting of two chromatographs connected via one electrically driven eight-port valve (Valco) and two storage loops was used.
- Evaporative light scattering detector (ELSD) PL-ELS 1000 from Polymer Laboratories

Chromatograph 1 (first separation step):

- Waters 2690 separation module Alliance.

Chromatograph 2 (second separation step):

- Waters 515 HPLC pump.

The software ‘PSS Win GPC7’ was used for data collection and processing and also controlled the operation of the coupled injection valves.

First Dimension (GEC):

- Supelco Nucleosil silica column: 100 Å, 5μm, 250x46(ID) mm.
- Eluent: the same gradient as for HPLC gradient analysis was used (gradient profile in 7.3)
- Flow rate: 0.115 mL/min

Second Dimension (SEC):

- PSS SDV Linear M column, 5 μm, 50x20(ID) mm.
- Eluent: THF
- Flow rate: 4 mL/min

The nebuliser and evaporator temperatures were set at 75 °C and 110 °C respectively and the rate of nitrogen flow was 1.5 SLM (standard liter per minute).

3.8.2 Solvents

Solvents used in the two-dimensional GEC-SEC analyses were solvent B (10% ethanol in toluene), cyclohexane and Chromasolve HPLC grade THF.

3.8.3 The solvent gradient

The gradient profile in Table 3.2 was used for all the two dimensional analyses in this study. This profile was determined to be the optimum for the first dimensional separation.

Table 3.2: Gradient profile used during 2D analysis in the first dimension

	% Solvent	
Time(min)	Solvent B	Cyclohexane
0	40	60
8.7	40	60
139	100	0
183	100	0
200	40	60

3.8.4 Sample preparation

All samples were prepared in exactly the same way as for the gradient elution HPLC analysis, except that higher concentrations were used (10 to 20 mg/mL).

3.9 Preparation of films – spin coating

Samples were dissolved in toluene and films were spin-coated on glass or aluminum slides. A model WS-400A-6NPP/LITE/10K spin coater of Laurel Technologies was used. A conventional oil pump was used for vacuum and N_2 gas to disperse the evaporating solvent. Samples were spin coated using a 1200 rpm spin speed.

3.10 Atomic force microscopy

AFM is an example of a SPM (scanning probe microscopy) technique, used to analyse polymer surfaces. The operating mode of all SPM's is similar – the forces acting between the probe and the sample are measured in all cases[7]. AFM is therefore based on the detection of atomic interaction forces between a sharp tip and the sample. By sampling the interaction force over a two-dimensional array, a topographic image with (sub)nanometer resolution is generated[8].

There are different modes in which the AFM instrumentation is operated. In contact mode, the probe is close to the sample and the interaction forces between the atoms of the sample and the atoms of the tip of the probe are repulsive. The distance between the probe and sample is larger in the non-contact mode and the interaction forces are attractive (van der Waals forces)[7].

In this study, the AFM was operated in the intermittent contact or tapping mode called digital pulsed force mode (DPFM). This mode combines both techniques mentioned above and generates a topographic image simultaneously with an image of the adhesion of the scanned area. The AFM is operated with a sinusoidal modulation applied to its *z*-piezo[8]. The modulation frequency is below the resonance frequency (f_r) of the cantilever - in this case the modulation amplitude was set to 1 kHz.

3.10.1 AFM instrumentation

All AFM measurements were made using a Veeco Multimode instrument with a Witec digital pulsed force mode controller. The images were recorded with a scan size of 2-5 μm x μm.

3.11 Static contact angle measurements

The hydrophobicity of different samples containing different ratios of PMMA to PDMS, as well as pure PMMA has been quantified using static contact angle measurements. Changes in hydrophobicity of the sample upon corona degradation were also monitored with this technique. Sample preparation involved the spin-coating of copolymer samples onto a glass slide. The analysis was done at room temperature with distilled water and the glass slides were mounted on a horizontal smooth surface. A 1μL (micro liter) syringe was used to place a droplet of a volume of 1μL on the polymer surface.

A magnified image was captured using a Nikon SMZ-2T (Japan), model VCC 250C digital video camera. PVR-plus software was used along with Able Image Analyser (μ-labs) version V3.6, which enabled calculation of the contact angles. The contact angle of the water droplet with the surface of the substrate was thus measured and reported as angle theta (θ). Figure 3.1 shows an example of the captured image. Included on the image are the parameters used to determine the static contact angle according to the relationship in equation 3.2.

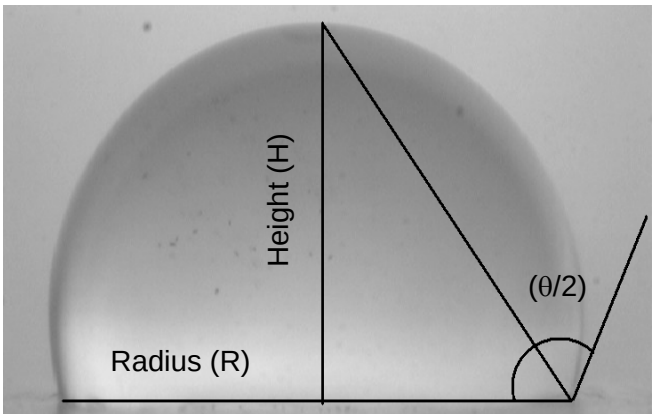

Figure 3.1: Image of water drop showing the height and radius used in determination of the contact angle θ.

$$\theta = 2\times\tan^{-1}(H/R) \qquad 3.2$$

Droplets were placed on different positions on the polymer sample and an average of 10 measurements was done per sample to eliminate the possible human reading error.

Images were taken directly after the specific droplet has been placed on the polymer surface. The actual contact angle was determined by analysing the dimensions of the droplet from the digital image.

3.12 Photoacoustic FTIR

FTIR is a common tool to analyse the chemical composition of a product and monitor the presence of certain chemical functionalities. PAS-FTIR has the advantage that no sample preparation is required and the sample can be scanned in whatever form it appears.

A Perkin Elmer Paragon 1000 FTIR was used to record spectra. The samples were placed in a MTEC 300 chamber and flushed with ultra high purity helium. The photoacoustic detector used was a MTEC model 300 unit coupled to the Perkin Elmer Paragon 1000.

The following parameters were used for the determination of each spectrum:

Mirror velocity (OPD)	=	0.15 m/s, 0.30 m/s, 0.05 m/s and 0.75 m/s
Resolution	=	8 cm^{-1}
Source aperture	=	maximum
Spectral Range	=	450 – 4 000 cm^{-1}
Number of scans	=	128
Sample reference	=	carbon black
Detector gas atmosphere	=	helium

A typical scan required fifteen minutes scan time. This allowed enough time for the sample temperature to equilibrate and hence, to obtain a quantitative measurement controlling the room temperature was not necessary.

3.13 Positron annihilation spectroscopy

Positron Annihilation Spectroscopy has become one of the most successful techniques for directly examining the free volume holes in polymers. A radioactive source such as Na^{22} emits positrons into the polymer matrix and become thermalised. These positrons

may annihilate with electrons or form a positronium (Ps). Positrons are anti-electrons, and when a positron collides with an electron, the two particles annihilate and their masses are converted into energy in the form of photons. The photons carry information on the electronic environment in which the annihilation occurred. This technique is recognised as a powerful tool in performing micro structural analysis of polymeric materials[9].

The positron beam results are reported as the S parameter or defect parameter in this study. It is calculated from the Doppler broadening energy spectra. The S parameter can be defined as the ratio of the central area to the total area of the annihilation peak after background subtraction. The S parameter can be related to the free volume hole sizes. This is presented in figure 3.2. The depth of penetration can be varied according to the relationship in equation 3.2[10], by varying the incident energy of the incoming positrons; Z is the depth penetrated (nm), E_+ is the incident energy (keV) and ρ is the density of the sample (kg/m^3).

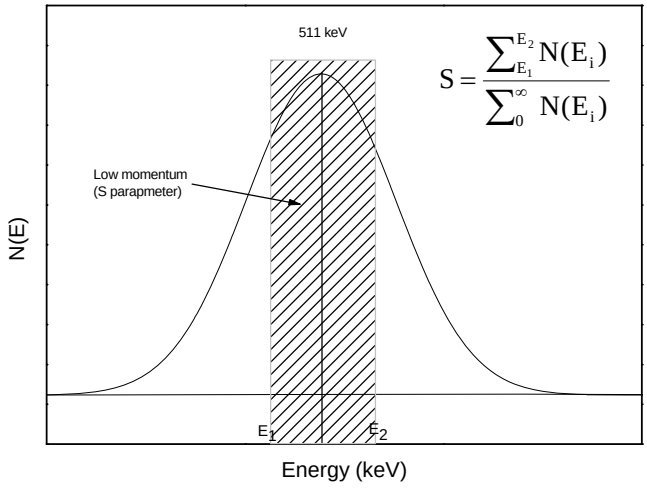

Figure 3.2: The Doppler broadening energy distribution of annihilation radiation and definition of the S parameter.

$$Z(E_+) = (400/\rho)E_+^{1.6} \qquad 3.3$$

The variable mono-energetic positron beam at the University of Missouri, Kansas City, USA was used for the sample analysis. Sample preparation was done as described in section 3.9.

3.14 Surface modification by corona treatment

PDMS samples were spin coated onto glass or aluminum slides. These samples were placed at the bottom of a one liter glass beaker to prevent dissipation of ozone into the atmosphere.

The samples were exposed to a very high frequency corona discharge in air at room temperature and normal atmospheric pressure for 30 minutes with a model BD-20AC of high frequency laboratory corona treated, supplied by Electro-Technic product, USA.

The distance between the stationary tip of the corona discharger and the surface of the PDMS sample is about 5 mm. The corona treater generates a spark of visible glow impinged to the surface of the sample for 30 minutes. The nature of the corona formed in the needle electrode corona treater is similar to the corona ageing that occurs during the in-service use of high voltage insulators.

The needle electrode has high ion bombardment which has a serious effect on the degradation of the material. A schematic diagram of the desk top corona discharger is shown in Figure 3.3.

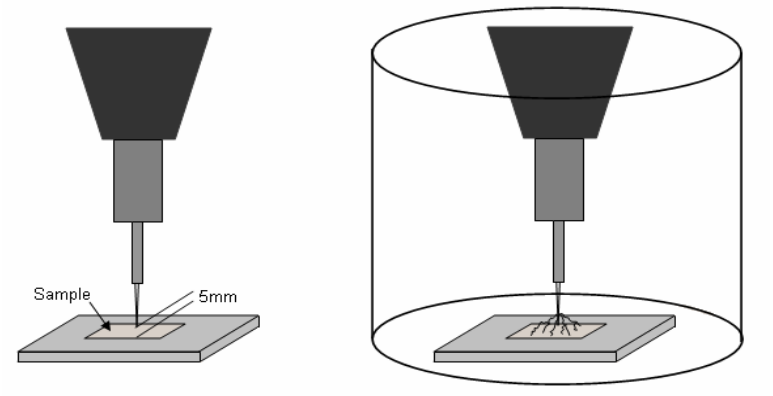

Figure 3.3: A schematic diagram of the desktop corona discharger showing tip to sample distance and operation in a glass beaker.

3.15 References

(1) Vogel, A. I. In *Chapter 4: Solvents and Reagents. Textbook of Practical Organic Chemistry.*; Pearson, Prentice Hall: England, 1989.

(2) Smith, S. D.; DeSimone, J. M.; Huang, H.; York, G.; Dwight, D. W.; Wilkes, G. L.; McGrath, J. E. *Macromolecules* **1992**, *25*, 2575-2581.

(3) Shinoda, H.; Miller, P. J.; Matyjaszewski, K. *Macromolecules* **2001**, *34*, 3186-3194.

(4) Boutevin, B.; Pietrasanta, Y.; Taha, M. *Makromol. Chem.* **1982**, *183*, 2977.

(5) Mera, A. E.; Goodwin, M.; Pike, J. K.; Wynne, K. J. *Polymer* **1999**, *40*, 419-427.

(6) Graef, S. M.; Van Zyl, A. J. P.; Sanderson, R. D.; Klumperman, B.; Pasch, H. *J. Appl. Polym. Sci.* **2003**, *88*, 2530-2538.

(7) Meincken, M.; Sanderson, R. D. *S. Afr. J. Sci.* **2004**, *100*, 256-260.

(8) Meincken, M.; Roux, S. P.; Jacobs, E. P. *Appl. Surf. Sci.* **2005**, *252*, 1772-1779.

(9) Jean, Y. C.; Mallon, P. E.; Zhang, R.; Chen, H.; Wu, Y.; Li, Y.; Zhang, J. In *Chapter 11: Applications of slow positrons to polymeric surfaces and coatings. Principles and applications of positron and positronium chemistry.*; Jean, Y. C.; Mallon, P. E.; Schrader, D. M., Eds.; World Scientific Publishing: Singapore, 2003.

(10) Cao, H.; Zhang, R.; Sundar, C. S.; Yuan, J. P.; He, Y.; Sandreczki, T. C.; Jean, Y. C. *Macromolecules* **1998**, *31*, 6627-6635.

Chapter 4

Results and Discussion

4.1 Synthesis of macromonomers

Several methods can be used for the PDMS macromonomer synthesis. The first method explored for the synthesis of the methacrylated-PDMS macromonomers in this project was by the functionalisation of a monohydroxy-terminated PDMS with methacryloyl chloride. This is an example of an esterification reaction by alcoholysis, which is the reaction between an alcohol and an acid halide. In this case the product of the esterification reaction would be the ester; methacrylated-PDMS and a quarternary ammonium salt. This method was found to be quite time-consuming and not very successful in using the synthesised macromonomers for graft copolymerisation. There was rather focused on the living anionic polymerisation of the macromonomers as described in Section 4.1.1.

4.1.1 Living anionic synthesis of macromonomers

Poly(dimethylsiloxane) macromonomers of various lengths with narrow molar mass distribution and controlled molar masses were synthesised through the utilization of living anionic ring-opening polymerisation of hexamethylcylclotrisiloxane(D_3). This study involved the functional termination of the living polymerisation with a chlorosilane derivative of allyl methacrylate to afford a methacryloxy-functionalised PDMS macromonomer[1]. The overall reaction scheme is shown in Scheme 4.1. The chlorosilane functional terminating agent was selected over the similar C-Cl compound since these are known to provide a higher functional termination. Details of the synthetic procedure can be found in Section 3.2.2. Great care needs to be taken in the synthesis since any traces of impurities such as moisture or air results in no reaction occurring.

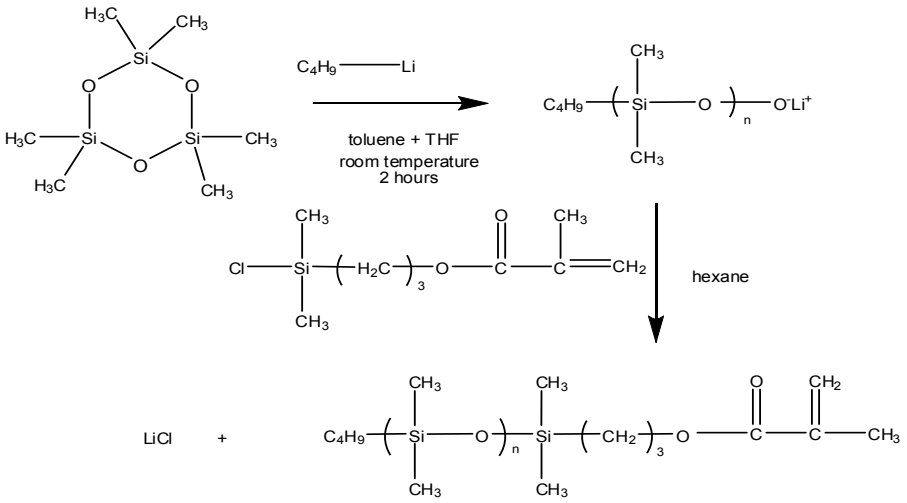

Scheme 4.1: Synthesis of the PDMS macromonomer.

4.1.2 Size exclusion chromatography results for synthesised macromonomers

With the anionic synthesis of macromonomers, a polydispersity index (PDI) close to one was obtained. These PDI values indicate the synthesis of very narrowly dispersed polymer chains. This can be attributed to the living nature of the anionic synthesis technique[2]. Table 4.1 contains information on the amount of monomer (D_3), initiator (butyllithium) and terminating agent (MPDC) that were used in the reactions for the synthesis of the PDMS macromonomer anionically. It must be noted that for the SEC there is no UV overlay, as PDMS does not have UV absorbing groups in this range of analysis. The use of an ELSD detector allowed detection of the polymer, since the refractive index of PDMS (1.43) is almost identical to that of THF (1.41)[3]. THF being the mobile phase in our SEC experiments, the differential refractive index (DRI) detector did not allow detection of the polymer. Any values for the PDMS are relative, since PS standards were used to calibrate the system.

Table 4.1: Results for synthesis of PDMS-macromonomers.

Reaction	D_3 monomer(g)	Butyllithium(mL)	MPDC(g)	M_n	M_w	PDI
AP1	4.99	0.6	0.575	1977	2165	1.09
AP2	3.01	0.5	0.41	1462	1658	1.13
AP3	5.00	0.1	0.57	2725	3849	1.41
AP4	4.98	0.1	0.55	5942	6251	1.05
AP5	4.99	0.1	0.57	4729	6207	1.31
AP6	7.07	0.1	0.82	6670	7049	1.06

PDMS-macromonomers with a low polydispersity index were obtained. The molar masses that were obtained were not always as calculated – probably due to a low functionality of the n-butyllithium that was used to initiate the ring-opening polymerisation. The PDI values also range between 1.05 and 1.41 which is a good indication of uniform chain growth.

4.1.3 NMR results of macromonomers

The formation of the PDMS-macromonomers from the living anionic polymerisation of D_3 was monitored by ^1H NMR by looking at the shift in the protons of hexamethylcyclotrisiloxane (D_3) and PDMS respectively[4]. The D_3 ring-opening was monitored with ^1H NMR by observing the decrease of the methyl peak of the cyclic monomer at a chemical shift of δ 0.128 ppm (b in figure 4.1) and the concurrent increase of the peak corresponding to the methyl protons of the linear species at δ 0.048 ppm. (a in Figure 4.1).

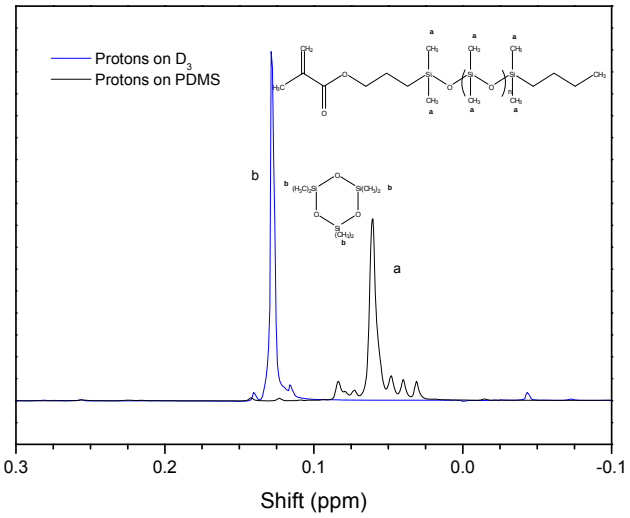

Figure 4.1: ^1H NMR spectra of D_3 monomer and PDMS polymer showing the shift in -CH_3 proton peak on polymerisation.

Proton NMR spectra of the reaction mixture were run as the reaction proceeded. From these ^1H NMR spectra it can be clearly observed that the PDMS peak increased and the

D_3 peak decreased as the reaction proceeded. Therefore it can be concluded that the cyclic monomer was successfully converted to PDMS-macromonomer.

The formation of the PDMS macromonomer by anionic polymerisation was confirmed by taking a ^{1}H NMR sample of the product. Peaks were clearly assigned and confirm the formation of the PDMS macromonomer. Figure 4.2 shows the PDMS macromonomer after the extraction of excess terminating agent and unreacted D_3 monomer. The vinylic peaks can be observed at 10a and 10b. A large peak can be observed at a shift of δ 0.05 ppm indicating the methyl peaks on siloxane.

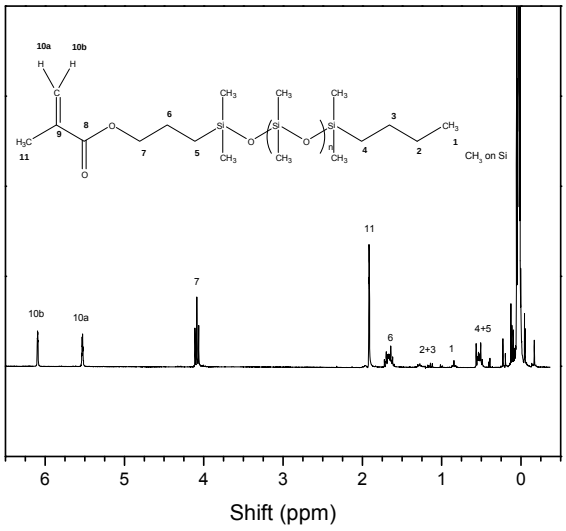

Figure 4.2: Typical ^{1}H NMR spectrum of monomethacryloxypropyl PDMS-macromonomer.

4.2 Synthesis of graft copolymers

4.2.1 Grafting reactions

The methacryloxy-functionalised macromonomers, having a range of molar masses, were copolymerised with methyl methacrylate to form graft copolymers of various chemical compositions. Copolymerisation of methyl methacrylate was carried out with PDMS macromonomers with number-average molar mass that varied from 1000 to 10 000 g/mol and the composition of the copolymer was varied from 1:48 to 1:500 (PDMS

macromonomer:MMA) molar ratio. Both commercial macromonomers, as well as macromonomers synthesised during the study anionically, were used in the copolymerisation of the graft copolymers. Scheme 4.2 shows the reaction used in the graft copolymer synthesis.

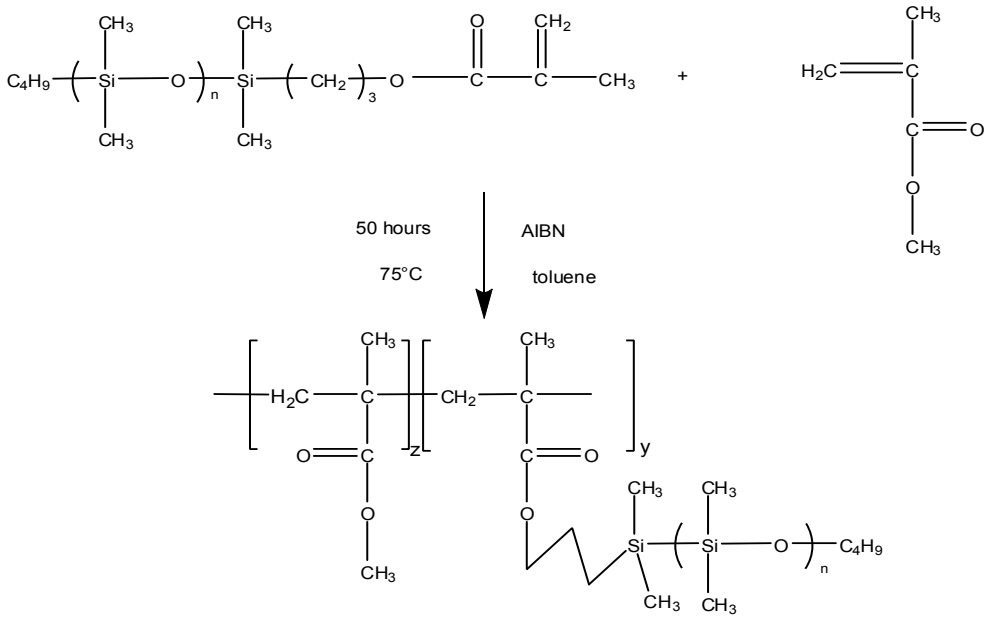

Scheme 4.2: Grafting reaction of PMMA-g-PDMS.

4.2.2 SEC results of the grafting reactions

The molar mass determinations of grafts copolymerised from MMA and PDMS macromonomers were done by size exclusion chromatography. Table 4.2 shows a summary of the graft copolymers synthesised with the commercially available macromonomers. The table summerises the copolymerisation feed ratios, the final product ratios and the molar mass data for the copolymers.

In the reactions GPS1 – GPS5, the short commercial macromonomers (Mn ≈1000) were used for the copolymerisation of the graft copolymers. Commercial macromonomers of medium length (Mn ≈ 5000) were used for GPM1 – GPM5 and long macromonomers (Mn ≈ 10 000) were used in GPL1 – GPL5.

Table 4.2: The SEC results of the graft copolymers prepared via the macromonomer method with commercial macromonomers [a]

Sample code	Macromonomer Length(M_n)	AIBN(mol)	Feed ratio(mol) [PDMS:MMA]	Product ratio[b] [PDMS:MMA]	M_n[c]	M_w[c]	PDI
GPS1	~1000	$1.1x10^{-4}$	1:25	1:21	34727	65844	1.9
GPS2	~1000	$1.3x10^{-4}$	1:48	1:36	9628	30848	3.2
GPS3	~1000	$1.5x10^{-4}$	1:100	1:47	16151	51552	3.19
GPS4	~1000	$3.2x10^{-4}$	1:300	1:86	17394	46432	2.67
GPS5	~1000	$1.5x10^{-4}$	1:500	1:26	31713	95701	3.02
GPM1	~5000	$4.1x10^{-5}$	1:25	1:7.5	6630	23168	3.49
GPM2	~5000	$8.6x10^{-5}$	1:48	1:3	45211	73243	1.62
GPM3	~5000	$1.1x10^{-4}$	1:100	1:65	25553	53323	2.09
GPM4	~5000	$1.8x10^{-4}$	1:300	1:70	16172	44860	2.77
GPM5	~5000	$1.5x10^{-4}$	1:500	1:141	35166	68895	1.96
GPL1	~10 000	$3.2x10^{-5}$	1:25	1:2	13426	14492	1.08
GPL2	~10 000	$6.1x10^{-5}$	1:48	1:18	21001	48497	2.31
GPL3	~10 000	$1.2x10^{-4}$	1:100	1:10	25570	53959	2.11
GPL4	~10 000	$9.9x10^{-5}$	1:300	1:82	26284	54369	2.07
GPL5	~10 000	$1.4x10^{-4}$	1:500	1:130	48013	74377	1.55

[a]Polymerisation conditions: PDMS macromonomer and MMA were reacted at 75°C in toluene for 48h with AIBN as initiator, a conventional free radical reaction.
[b]The ratio represents the PDMS-MA/ mol fraction MMA in the copolymer determined by proton NMR (see section 2.2)
[c]Values reported relative to polystyrene standards used in the calibration

SEC results can be compared as a function of macromonomer length or as a function of feed ratio. PDMS:PMMA ratios in the graft copolymer show a clear trend to the feed ratio of PDMS:PMMA. The physical content of final graft products also corresponds to the PDMS:PMMA ratios – graft copolymers that has a very high amount of PDMS incorporated is not a solid polymer, but consists of a thick, viscous liquid. The product ratios of the final graft copolymer was determined with ^{1}H-NMR and full details of peaks used in the integration and δ shifts is given in Section 4.2.2. These product ratios were determined after the extraction of unreacted PDMS-macromonomer from the final product with hexane.

SEC results of grafts copolymerised from anionically synthesised macromonomers are shown in Table 4.3. Short macromonomers (Mn ≈ 1000) were used in the reactions GPS6 – GPS8 and macromonomers of medium length (Mn = 5000) were used in reactions GPM6 – GPM8. The ratio of PDMS:PMMA in the final copolymer corresponds to the initial feed ratios. An increasing amount of PMMA incorporated into the graft

copolymers as intended by the feed ratio can be clearly observed for the series where medium length (Mn ≈ 6670) macromonomers were used.

Table 4.3 The SEC results of graft copolymers prepared via the macromonomer method with synthesised macromonomers[a]

Sample code	Macromonomer length(M_n)	AIBN(mol)	Feed ratio(mol) [PDMS:MMA]	Product ratio[b] [PDMS:MMA]	Mn[c]	Mw[c]	PDI
GPS6	1462	$3.7x10^{-5}$	1:25	1:7	23095	82382	3.57
GPS7	1977	$5.7x10^{-5}$	1:48		57759	87067	1.51
GPS8	2725	$9.4x10^{-5}$	1:100	1:6	308	328	1.07
GPM6	6670	$1.2x10^{-5}$	1:25	1:5	6634	7429	1.12
GPM7	6670	$2.2x10^{-5}$	1:48	1:14	14297	71111	4.97
GPM8	6670	$2.4x10^{-5}$	1:100	1:29	9547	95041	9.95

[a]Polymerisation conditions: PDMS macromonomer and MMA were reacted at 75°C in toluene for 48h with AIBN as initiator, a conventional free radical reaction.
[b]The ratio represents the PDMS-MA/ mol fraction MMA in the copolymer and was calculated using ^{1}H NMR (see section 2.2)
[c]Values reported relative to polystyrene standards used in the calibration

4.2.3 NMR results of the grafting reactions

^{1}H-NMR was done on the twice extracted co-polymer. This was done to ensure the full removal of any unreacted PDMS macromonomer. (This is further discussed in Section 4.3.1) The presence of the PDMS peaks in the spectra confirms graft formation – illustrating that the PDMS must have been incorporated into the graft, since all of the unreacted PDMS-macromonomer has been extracted. The PDMS-macromonomer was extracted from the graft copolymer by stirring the precipitated reaction mixture over hexane twice, for 24 hours. Successful extraction of the unreacted macromonomer was monitored by gradient elution chromatography (GEC) (discussed in Section 4.31). Figure 4.3 shows a typical ^{1}H-NMR spectrum for the extracted graft copolymer.

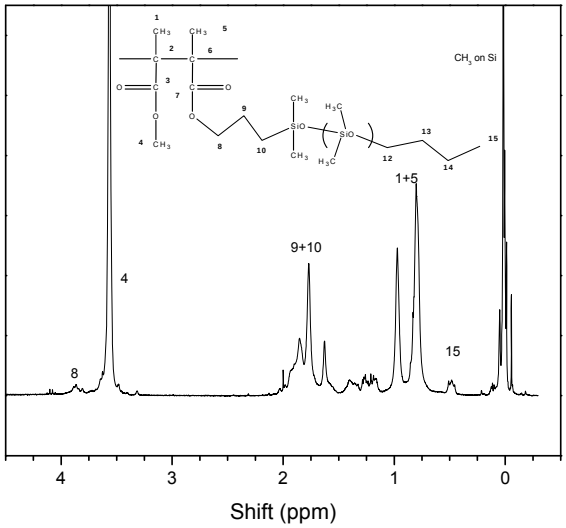

Figure 4.3: ^{1}H NMR spectrum of PMMA-g-PDMS.

The macromonomer content in the final graft copolymer was calculated by comparing integrated peaks of the ^{1}H NMR spectra relating to PMMA and the PDMS macromonomer respectively. The peak at δ 3.56 ppm corresponding to proton 4 and the peak at δ 0.5 ppm corresponding to proton 15 were compared. Peak 15 represents PDMS and peak 4 represents PMMA and these specific peaks were used due to the fact that they could be clearly assigned to PDMS and PMMA respectively. The results of the product ratios in the graft copolymers are shown in Table 4.2 and Table 4.3.

4.3 Liquid chromatography analysis

4.3.1 Gradient elution results

In gradient elution chromatography, monomers or polymers are eluted according to their chemical composition and corresponds to a specific elution volume or retention time. These analyses were done on the synthesised graft copolymers, as well as PDMS macromonomers and PMMA standards in order to evaluate the chemical composition of the synthesised graft copolymers. This technique was also used to monitor the efficiency of the extraction process and further prove graft copolymer formation.

Gradient elution chromatography of the macromonomers and grafts were done, as well as a range of PMMA-standards to evaluate where the relevant homopolymers and graft copolymers will elute. A gradient profile had to be developed in order to get the specific gradient where the copolymers and macromonomers would separate best. In order to achieve this, PMMA standards and macromonomers were eluted using different gradient profiles. The gradient profile shown below gave the best separation. The two solvents used in the gradient elution were cyclohexane (solvent A) and solvent B which consists of 10% ethanol in toluene. The gradient profile used is illustrated in Figure 4.4.

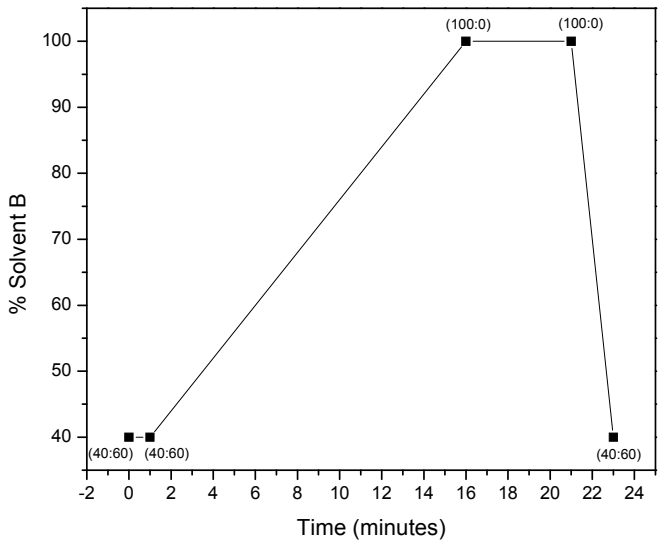

Figure 4.4: Solvent gradient profile used for GEC analysis with % solvent B (10% ethanol in toluene), plotted against time, solvent A is cyclohexane.

The solvent composition was increased to 100% solvent B (10% ethanol in toluene) within 16 minutes and was maintained at this composition for 5 minutes. As can be seen in figure 4.5, the PDMS macromonomer has a retention time of about 3 minutes. All the macromonomers elute at this volume irrespective of their molar mass.

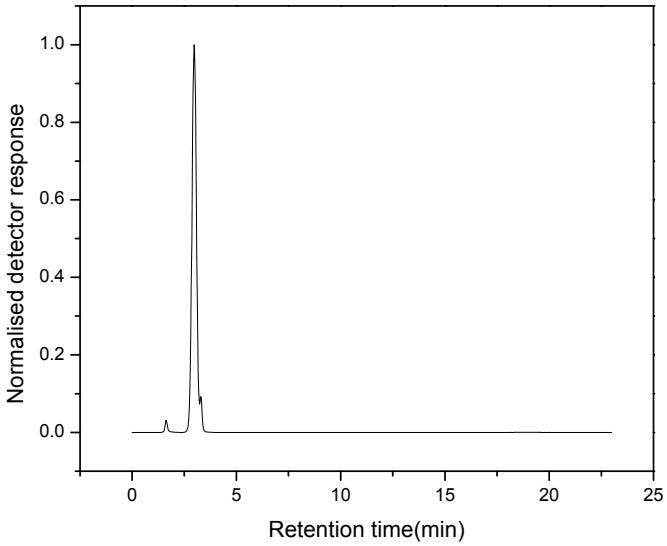

Figure 4.5: Gradient elution chromatogram of PDMS-macromonomer.

PMMA standards of increasing molecular mass were eluted and the results are shown in Figure 4.6 and an increase in retention time can be detected upon increasing molar mass.

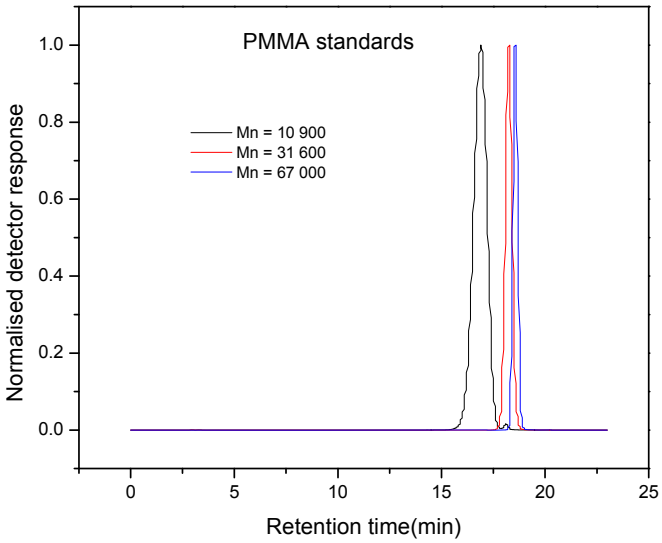

Figure 4.6: Gradient elution chromatogram of PMMA-standards.

It can be clearly seen that PDMS elutes first and PMMA only elutes later. This can be attributed to the relative polarity of the solvents and the components that are eluted. The polar PMMA elutes at a stage in the gradient elution profile when there is a 100% of the polar solvent, solvent B present and consequently the non-polar PDMS macromonomer is eluted at a much earlier stage of the gradient profile, when the solvent composition is still less polar due to a higher percentage of the non-polar cyclohexane being present.

Figure 4.7 shows the gradient elution chromatogram of GPS2 just after completion of the grafting reactions. The copolymer as well as residual PDMS-macromonomer is shown in the chromatogram for the sample that has just been precipitated in methanol. The PDMS macromonomer was extracted with hexane from these samples, by stirring the sample in hexane for 24 hours. The polymer was extracted with hexane for a second time to remove all of the residual macromonomer. It can be seen that the PDMS macromonomer has been extracted from the graft copolymer successfully by the decrease and virtual disappearance of the macromonomer peak at about 3 minutes retention time after extration. The width of the peaks also indicates chemical composition distribution – a broader peak indicating a larger distribution in chemical composition. This phenomenon will be fully investigated by two dimensional chromatography in Section 2.4.

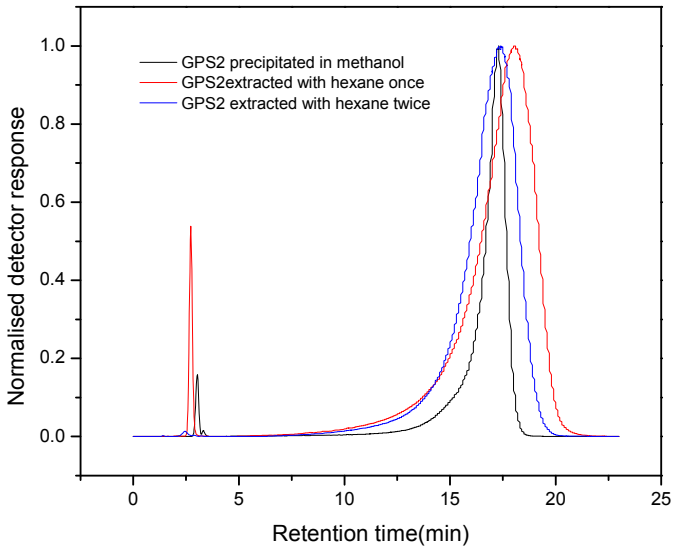

Figure 4.7: Gradient elution chromatogram of graft copolymer to show extraction of PDMS-macromonomer.

The PMMA-graft-PDMS copolymer elutes between 15 and 20 minutes. A shift to the left, therefore indicates a higher amount of PDMS in the copolymer and the copolymer has a lower elution volume. Different amounts of PDMS were incorporated into the graft copolymers synthesised in this study. Figure 4.8 shows the gradient elution profile of a series of the synthesised graft copolymers. For the reaction GPS1, the ratio of PDMS:PMMA was 1:25 and the amount of PMMA was increased gradually to a ratio of 1:300 for GPS4. The incorporation of PDMS into the graft copolymers was according to the feed ratios mentioned. The graft copolymer with the highest amount of PDMS will elute first and the graft copolymer with the lowest amount of PDMS will have the highest elution volume. Therefore, GPS1 is eluted first, followed by GPS2 and GPS3. The copolymer with the lowest amount of PDMS incorporated, GPS4 elutes last or at a longer retention time.

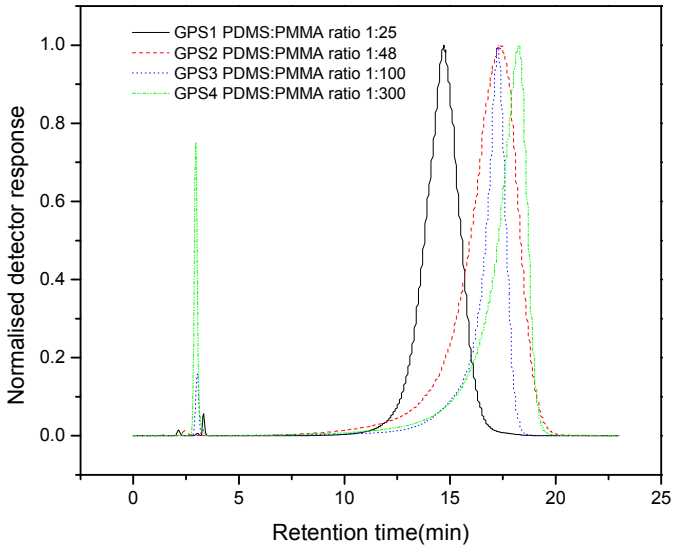

Figure 4.8: Gradient elution chromatogram to show influence of PDMS:PMMA ratio on elution volume.

In another set of reactions, the PDMS:PMMA ratio was kept constant, but the length of the PDMS macromonomer incorporated into the graft copolymer was varied. As the length of the PDMS macromonomer incorporated increases, an increased amount of PDMS is incorporated into the copolymer, and therefore the copolymers containing more PDMS are expected to elute earlier. This is shown in Figure 4.9, as the graft copolymer

grafted from the long macromonomer has more PDMS incorporated into the copolymer and therefore elutes before the graft copolymerised from the medium macromonomer.

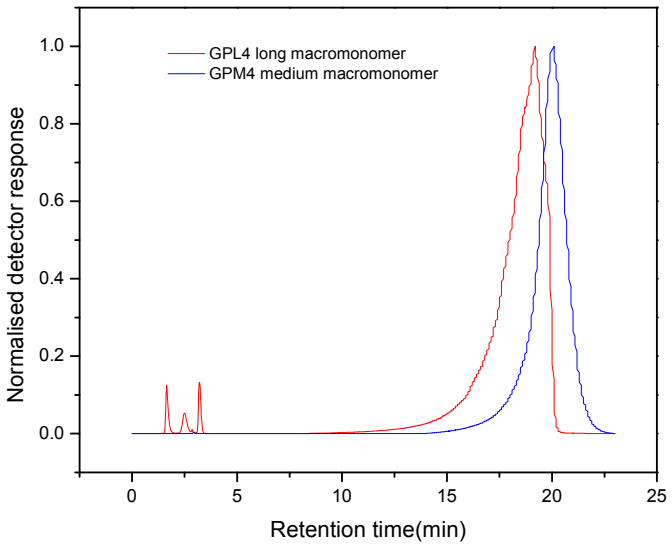

Figure 4.9: Gradient elution chromatogram to show the influence of macromonomer length on elution volume.

4.3.2 Two dimensional chromatography (GEC-SEC)

Samples were separated according to chemical composition via gradient elution chromatography in the first dimension and according to molar mass (by SEC) in the second dimension. Samples were eluted in the first dimension using the gradient as shown in Section 2.3 and fractions were injected into the second separation step via an online storage loop. These fractions that have now been separated according to chemical composition were injected into the second dimension and separated according to hydrodynamic volume by SEC. The fact that this particular combination has been used for the two-dimensional analysis can be highlighted, since this is not a very commonly used technique. Gradient elution chromatography has been used in the first dimension to separate molecules according to chemical composition via gradient analysis. Liquid chromatography at critical conditions (LCCC) is the most commonly used technique for separation in the first dimension. By working at the LCCC conditions of one of the components, this component is made invisible, therefore not contributing to the retention and allows the other component to elute[5]. This mode is slightly more

favourable for separation in the first dimension due to the fact that there is an isocratic solvent; therefore the composition of the solvent stays the same throughout the analysis in the first dimension. In this study the gradient profile in the first dimension makes the two dimensional analysis more difficult.

Figure 4.10 shows the two dimensional GEC-SEC chromatogram of the PMMA-g-PDMS grafting reaction. Two dimensional samples of the polymer that has been extracted twice, have been eluted. Two peaks can be observed and therefore this shows that both PMMA-homopolymer and a PDMS-graft-PMMA copolymer have been synthesised. Peak 1 can be attributed to PMMA homopolymer that has formed during the reaction. The graft copolymer PMMA-g-PDMS will elute earlier, at a lower elution volume as shown in the gradient analysis chromatograms in Section 4.3.1 and therefore peak 2 in the chromatogram can be assigned to be the graft copolymer, PDMS-g-PMMA. This grafting reaction clearly indicates a relatively large amount of PMMA homopolymerisation. In this reaction the long macromonomer was used. The large amount of homopolymerisation would have taken place due to the bulkiness of the long macromonomer. Despite this, a very clear peak indicative of graft formation can be seen. In this case the graft constitutes about 42% of the total area (amount of material) in the chromatogram.

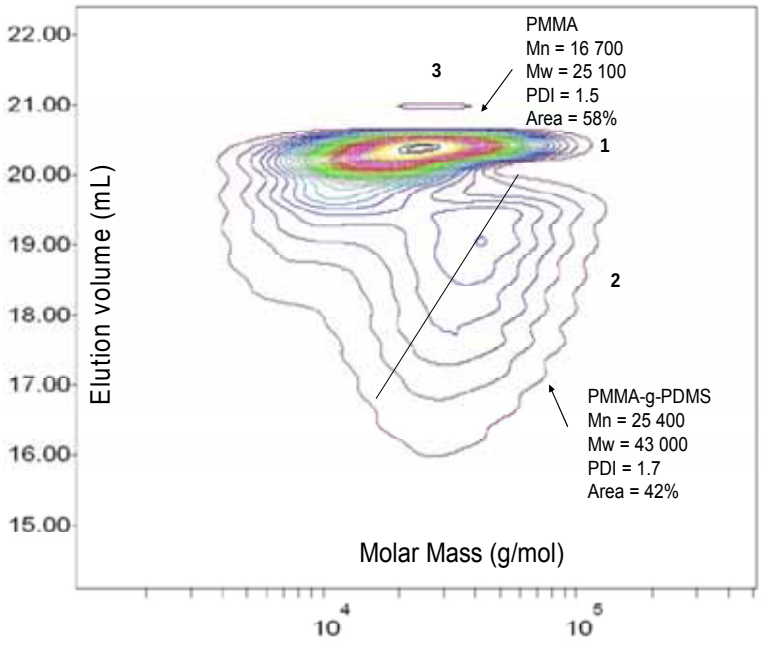

Figure 4.10: 2D Chromatogram of reaction GPL4. PMMA-g-PDMS copolymer with initial ratio of PDMS:PMMA 1:300 and PDMS macromonomer of Mn = 10 000.

Figures 4.11 and 4.12 show the 2D chromatograms of the graft copolymer polymerised with the short macromonomer. In this case little to no PMMA homopolymer is formed and only one peak is observed. The GEC-SEC results indicate that the molecules with the higher PDMS content (lower retention time in the first dimension) also have a relatively lower molar mass. This is indicated by the line in the two-dimensional plots. This may be a result of the inclusion of the bulky macromonomer in the chain reducing the overall molar mass of the higher graft content molecules.

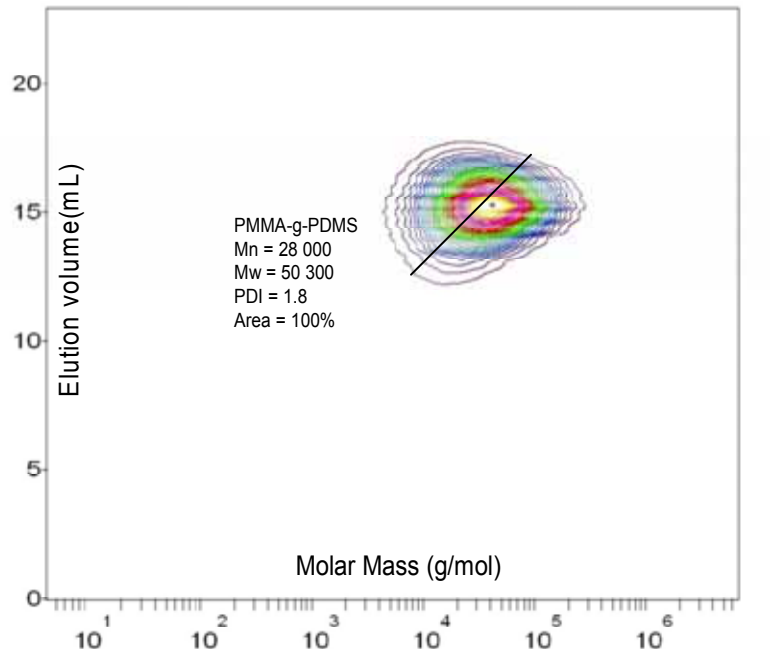

Figure 4.11: 2D Chromatogram of reaction GPS1. PMMA-g-PDMS copolymer with initial ratio of PDMS:PMMA 1:25 and PDMS macromonomer of Mn = 1000.

In Figures 4.11 and 4.12 the short macromonomers has been used and no homopolymerisation can be detected in this case compared to the reaction in figure 4.10. This can be attributed to the fact that the short macromonomer is a lot less bulky than the long macromonomer and chain movement would take place a lot more readily. In these two chromotograms, the GEC-SEC results also indicate that the molecules with the higher PDMS content (lower retention time in the first dimension) also have a relatively lower molar mass. This is indicated by the line across the 2D-plot. Again, this may be a result of the inclusion of the bulky macromonomer in the chain reducing the

overall molar mass. Generally the longer macromonomer series show some degree of PMMA homopolymerisation while this is not evident in the short macromonomer series.

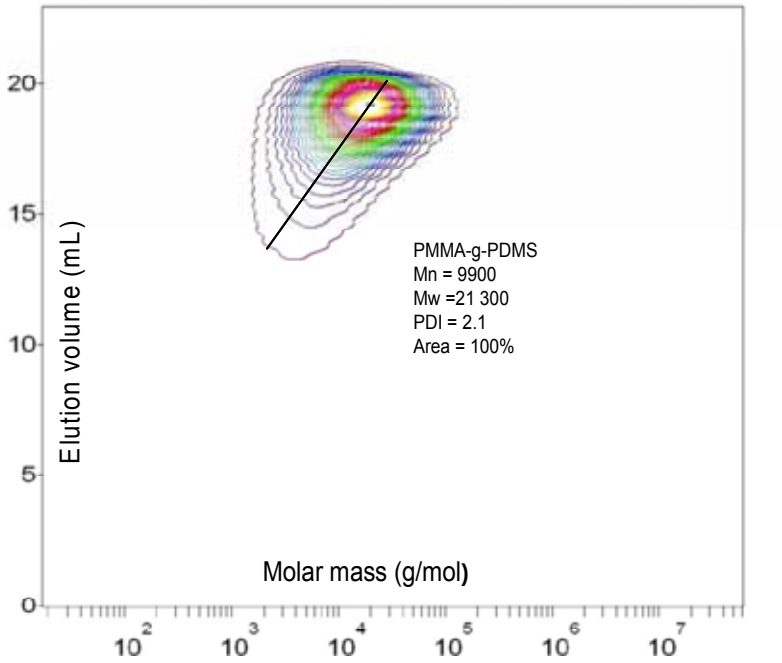

Figure 4.12: 2D Chromatogram of GPS2. PMMA-g-PDMS copolymer with initial ratio of PDMS:PMMA 1:48 and PDMS macromonomer of Mn = 1000.

4.4 Surface segregation and morphological studies

PDMS has very interesting surface properties after corona treatment and also shows the phenomenon of surface segregation when blended with organic polymers. This section of the study will focus on the properties of the graft copolymers after corona treatment as well as show PDMS surface segregation.

4.4.1 Contact angle measurements

PDMS shows high static contact angles with water droplets, due to its hydrophobic nature. PMMA has a lower contact angle of approximately 75˚. The first and simplest way to detect successful segregation of PDMS to the surface of the polymer sample is to measure the contact angles. Films of the graft copolymers were prepared by spin-coating onto glass slides. Contact angles of the graft copolymers were also determined

to investigate the effect of PDMS:PMMA ratio on the surface contact angles. PDMS is more hydrophobic than PMMA and therefore it is expected that contact angles would increase with increasing PDMS content in the graft copolymers. PDMS content is increased both by increasing the macromonomer length and increasing the amount of PDMS vs PMMA incorporated into the copolymers.

Contact angles measured for the graft copolymers are shown in Table 4.4 and 4.5. There is not much difference between samples, as the incorporation of PDMS in the graft copolymer changes. The expected increase in contact angle upon heating of the graft copolymers is also not really observed for the samples. This indicates that PDMS has already migrated to the surface of the samples during the spin-coating of the films. All of the graft copolymers, however, have a larger contact angle than pure PMMA due to the presence of the more hydrophobic PDMS in the copolymers. The results show that in most cases the surface contact angle is very close to that of the pure PDMS polymer, regardless of the copolymer composition. This indicates the strong surface segregation preference of the PDMS component in the copolymer[6]. This is further discussed in the slow positron beam analysis section where the surface segregation is further analysed.

Table 4.4: The surface contact angle results for the various graft copolymers copolymerised from commercial macromonomers.

Sample code	Ratio PDMS:PMMA in copolymer	Macromonomer length	Contact angle(θ)
GPS1	1:21	short	110.5
GPS1 heated[a]	1:21	short	106.3
GPS2	1:36	short	110.9
GPS3	1:47	short	107.8
GPS3 heated[a]	1:47	short	108.6
GPS4	1:86	short	107.1
GPS4 heated[a]	1:86	short	107.6
GPS5	1:26	short	113.9
GPM2	1:3	medium	90.5
GPM3	1:65	medium	113.3
GPM4	1:70	medium	67.2
GPL1	1:2	long	91.0
GPL3	1:10	long	114.7
GPL4	1:82	long	110.9
GPL4 heated[a]	1:82	long	112.7
GPL5	1:130	long	113.9

[a]Samples were heated overnight at 100˚C to promote further surface segregation of PDMS

Table 4.5: Contact angle measurements of graft copolymers copolymerised from synthesised macromonomers.

Sample code	Ratio PDMS:PMMA	Macromonomer length	Contact angle(θ)
GPS6	1:7	short	96.8
GPM6	1:5	medium	106.1
GPM7	1:14	medium	95.8
GPM8	1:29	medium	103.9

After corona treatment of the PMMA-g-PDMS samples, the normally hydrophobic nature of the PDMS surface switches to hydrophilic. This indicates that corona treatment leads to drastic changes in the surface structure of the PDMS layer. Directly after corona treatment, contact angles cannot be measured due to the water droplet just spreading on the surface due to this drastic change. This hydrophilic character is lost with time and the samples regain its hydrophobic character. The hydrophobicity recovery with time after corona treatment for the PDMS–g-PMMA copolymers is shown in figure 4.13.

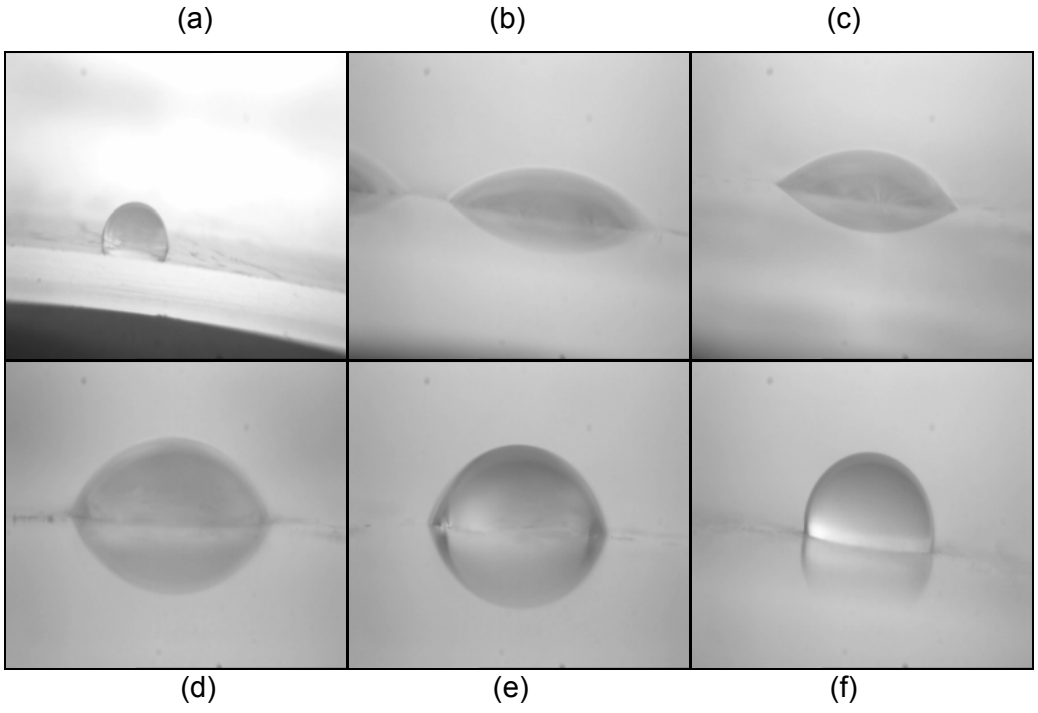

Figure 4.13: Contact angle recovery after corona treatment for GPS4. (a) Measured before corona treatment (b) 20 hours after corona (c) 24 hours after corona (d) 44 hours after corona (e) 116 hours after corona (f) 312 hours after corona treatment.

Contact angle data indicates a drastic change in the surface structure of the graft copolymers after corona treatment. There is an initially rapid recovery in the SCA after corona treatment but the rate of recovery slows down at longer times after treatment. This study has shown that PMMA-g-PDMS hybrid copolymers exhibit the phenomenon of hydrophobic loss and recovery after corona treatment similar to pure PDMS polymers. This is one of the first reported examples of a hydrophobicity recovery process occurring in PDMS containing hybrid materials. Bayley and Mallon[7] have also recently shown that polystyrene-block-PDMS copolymers also show this hydrophobocity recovery phenomenon. The mechanism of hydrophobicity loss and recovery is most probably very similar to the process involved in pure PDMS compounds because of the surface segregation of the PDMS component. In pure PDMS compounds the process of loss and recovery is explained by the degradation of the PDMS materials to form a glassy SiOx layer at the surface. This hydrophilic layer once again becomes hydrophobic due to the diffusion of low molecular weight silicone compounds formed *in-situ* during the degradation process back to the surface. The hydrophobicity recovery phenomenon after corona treatment for pure PDMS samples is fully documented and the mechanisms responsible for this recovery as well[8]. Further analysis was done to confirm and investigate this phenomenon and is discussed in Section 4.4.3 and Section 4.4.4.

Table 4.6 shows the contact angles of the sample before corona exposure as well as the contact angle 312 hours after corona treatment. It can also be observed that these samples do not regain their full hydrophobicity during this time. This is indicative of the fact that the corona exposure causes permanent materials changes. This is later confirmed in the slow positron beam analysis of the samples.

Table 4.6: A summary of the contact angle data of several corona treated sample films.

Sample code	Ratio PDMS:PMMA	Contact angle(θ) before corona	Contact angle(θ) 312hrs after corona[a]
GPS1	1:21	110.5	73.2
GPS2	1:36	110.9	74.9
GPS3	1:47	107.8	83.6
GPS4	1:86	107.1	66.4

[a]Samples were exposed to 30min corona discharge

The PMMA-g-PDMS hybrid material clearly exhibits a loss in hydrophobicity upon corona treatment and the recovery thereof similar to pure PDMS polymers. This is clearly shown in Figure 4.14.

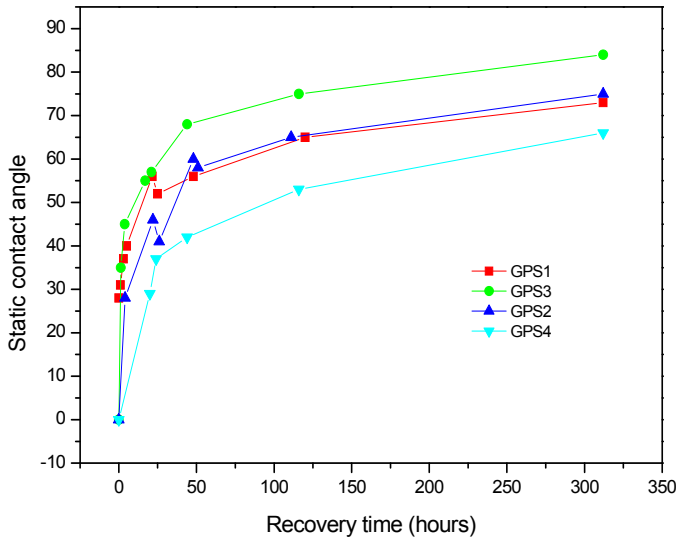

Figure 4.14: Hydrophobic recovery plotted against time for graft copolymer samples

4.4.2 Atomic force microscopy

AFM was used to evaluate the influence of the PDMS side chain length, and the PDMS:PMMA ratio on hydrophobicity, as well as to look at the influence of heating on the hydrophobicity of samples. Imaging and digital pulsed force mode (DPFM) measurements were performed with a silicon tip, which is slightly hydrophilic. An increase in adhesive force between the sample and the tip therefore relates to an increasing hydrophilicity (less hydrophobic) of the sample surface.

The graft copolymer consists of a PMMA backbone with hydrophobic PDMS side chains. Two different copolymers were analysed in order to look at the effect of heating on the hydrophobicity of samples, as well as to evaluate the influence of the PDMS side chain length on hydrophobicity and surface morphology. Heating should enhance the phase separation and lead to a more hydrophobic surface.

Firstly, a sample of GPM7 was analysed. The macromonomer used to synthesise the graft copolymer was of medium length; M_n≈5000 and the ratio of PDMS:PMMA is 1:48.

(a) (b)

Figure 4.15: AFM topography image of GPM7. Image (b) was heated.

Figure 4.15(a) shows the AFM topography image of the sample that was not heated. There are small surface structures visible on the surface. The surface roughness in this case was respectively 1.1nm (2µm scan size) and 3nm (5µm scan size). There is a large difference in adhesive force for the 2 different scan areas (light and dark), showing that the surface is not very homogeneous. The adhesive force observed for the sample varied between 27±2.5 nN (2µm) and 56±3.2 nN (5µm) with an average of approximately 42 nN.

Figure 4.15(b) shows the AFM topography image of the sample that was heated. There is a dramatic change in the surface after heating the sample. The larger features observed in the unheated sample have disappeared. The heated sample shows darker areas within the polymer surface and can be related to the phase segregation morphology expected in these materials. The surface roughness is 2.4nm (2µm scan size). The adhesive force observed for the sample is 22±5.2 nN. Heating seems to increase the surface roughness and slightly decrease the adhesive force. This means

that the surface becomes more hydrophobic upon heating of the sample due to phase separation taking place.

A sample of GPL5 was also analysed. This graft copolymer has long PDMS chains (M_n≈10 000) and the ratio of PDMS:PMMA is 1:500.

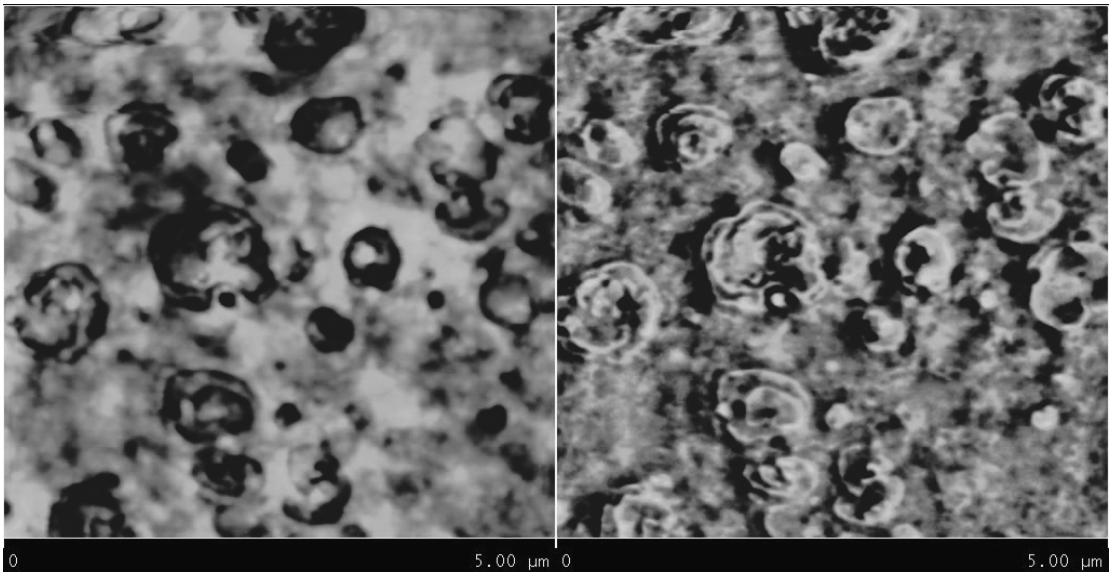

(a) (b)

Figure 4.16: AFM topography image of GPL5. Image (b) was heated.

Note the completely different surface structure for figure 4.16(a); the sample that was not heated. The surface features show large round structures on the surface. The surface roughness for figure 4.16(a), the sample that was not heated, was 6.5 nm (2µm scan size) and the adhesive force 104±11.3 nN (2µm scan size).

The surface roughness is recognisably larger than for GPM7, which can be explained by the large structures on the surface. The adhesive force is about 3 times larger, which means that the surface of GPM7 is generally a lot more hydrophobic than GPL5. This can be attributed to the larger ratio of PDMS incorporated into the graft copolymer of GPM7 and the higher PDMS content at the surface.

In Figure 4.16(b), the sample that was heated, the surface roughness is 4 nm (2 µm scan size) and 4.4 nm (5µm scan size). The adhesive force is respectively 55±9 nN (2 µm) and 67±8.1 nN (5 µm). The adhesive force values are in a close range and indicate

that heating only slightly increases the surface hydrophobicity. In this case it also decreases the surface roughness.

A larger set of samples were analysed to evaluate the influence of the PDMS side chain length, as well as the PDMS:PMMA ratio on hydrophobicity. The following four sample sets were analysed:

Sample set 1: spin coated
Sample set 2: spin coated and heated
Sample set 3: film on Si
Sample set 4: film on Si and heated

Two different sets of samples were prepared as shown above. A set of 5 graft copolymers with short side chains and decreasing PDMS:PMMA ratio were compared. In the second set, the PDMS:PMMA ratio was kept constant at 1:100 and the side chain length was varied from short to long.

Table 4.7: The sample range used in AFM analysis is highlighted in the table below.

Sample code	Macromonomer length	Feed ratio(mol)
GPS1	short	1:25
GPS2	short	1:48
GPS3	short	1:100
GPS4	short	1:300
GPS5	short	1:500
GPM1	medium	1:25
GPM2	medium	1:48
GPM3	medium	1:100
GPM4	medium	1:300
GPM5	medium	1:500
GPL1	long	1:25
GPL2	long	1:48
GPL3	long	1:100
GPL4	long	1:300
GPL5	long	1:500

All samples with phase separation indicate that PDMS tends to segregate to the surface and sometimes even forms spherical structures on the surface (hydrophobic = dark in the adhesion image). Some films had holes, which were mostly more hydrophilic, which suggests that the PMMA forms the bulk of the film and the PDMS side chains the surface layer.

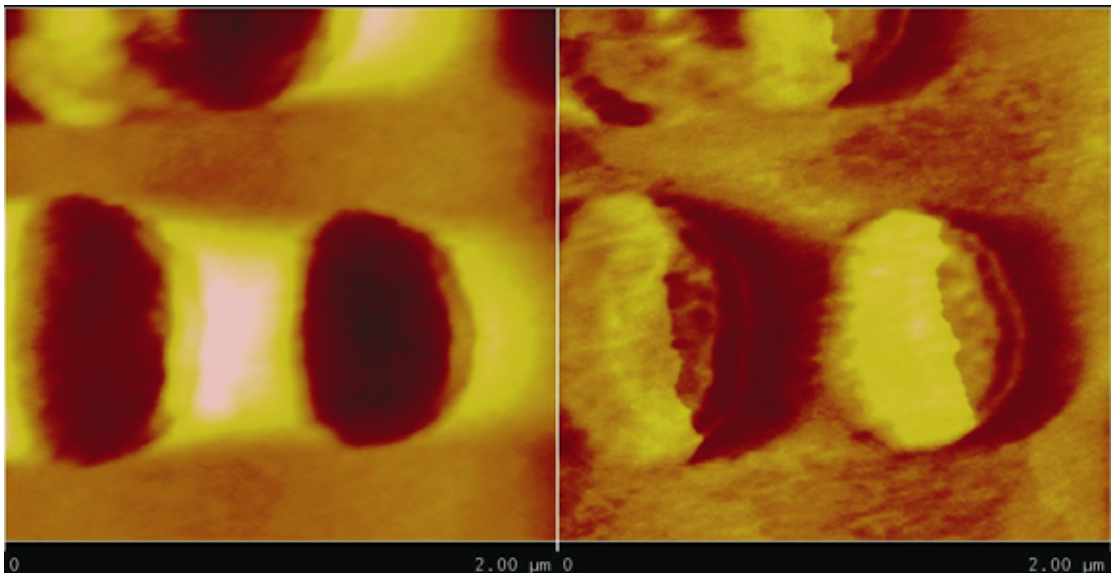

(a) (b)

Figure 4.17: GPS4 with short PDMS side chains and PDMS:PMMA ratio of 1:300; (a) topography and (b) adhesion. Holes in the topography are lighter areas (=more hydrophilic) in the adhesion image.

This is clearly seen in figure 4.18 where the topographical image shows rounded type structures on the surface and the adhesive force image indicates that these are PDMS domains since they appear as darker areas (more hydrophobic).

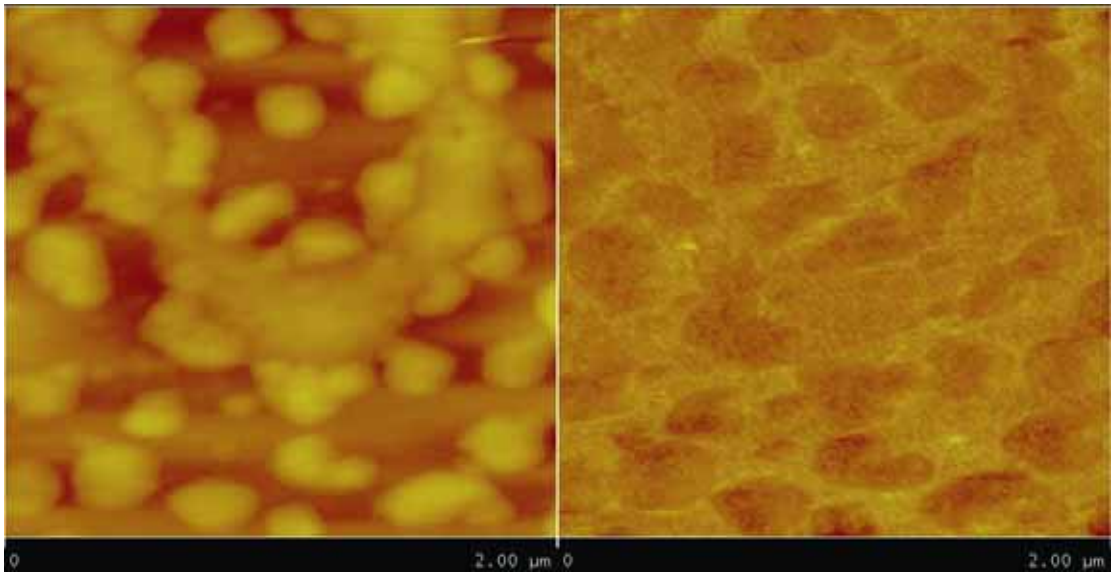

(a) (b)

Figure 4.18: GPS5 with short PDMS side chains and PDMS:PMMA ratio of 1:500; (a) topography and (b) adhesion.

Figure 4.19 shows the effect of thermal treatment on the surface morphology of the polymers. The thermal treatment increases the number of spherical features on the

surface and indicates a more ordered phase morphology which is richer in the hydrophobic PDMS component.

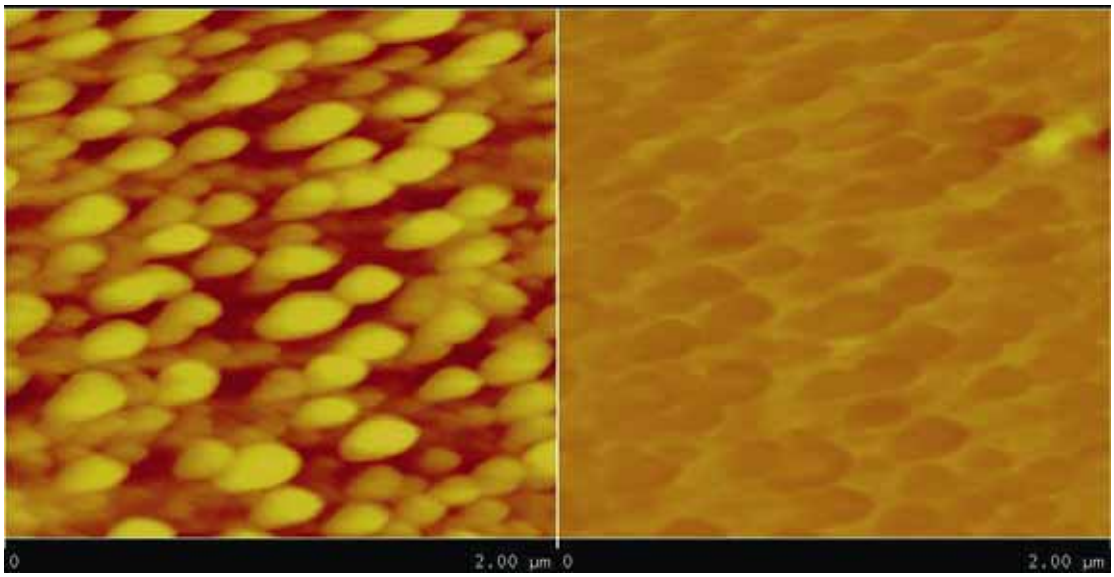

(a) (b)

Figure 4.19: GPS5 with short PDMS side chains and PDMS:PMMA ratio of 1:500 after heating; (a) topography and (b) adhesion.

Figure 4.20 and 4.21 show the adhesive force as a function of the PMMA content. Although there is a large amount of scatter in the data it can be seen that there is a generally increasing adhesive force with PMMA content. The large amount of scatter may be due to the distribution of the surface features seen in the previous topographical images. Nevertheless the results indicate a relationship between the amount of PDMS surface segregation and the PDMS content in the polymer. It is interesting to note that while the AFM results suggest a heterogeneous distribution on the surface, the contact angle measurements show less dependence on the copolymer composition and thermal treatment.

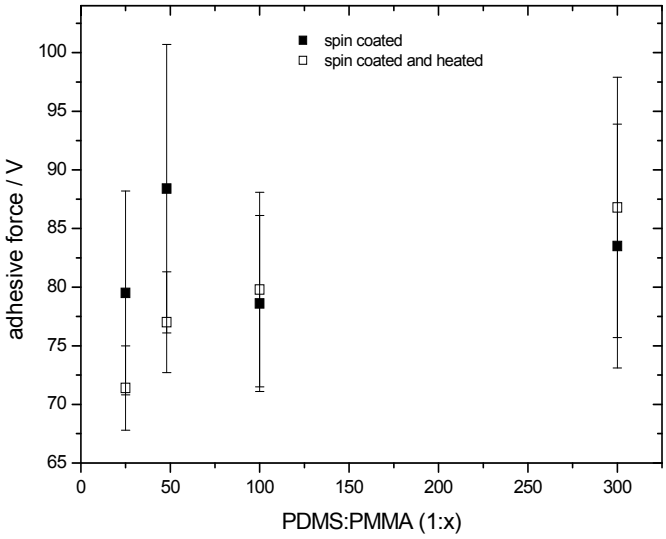

Figure 4.20: Change in surface polarity (as determined by the adhesion force) with increasing PMMA content.

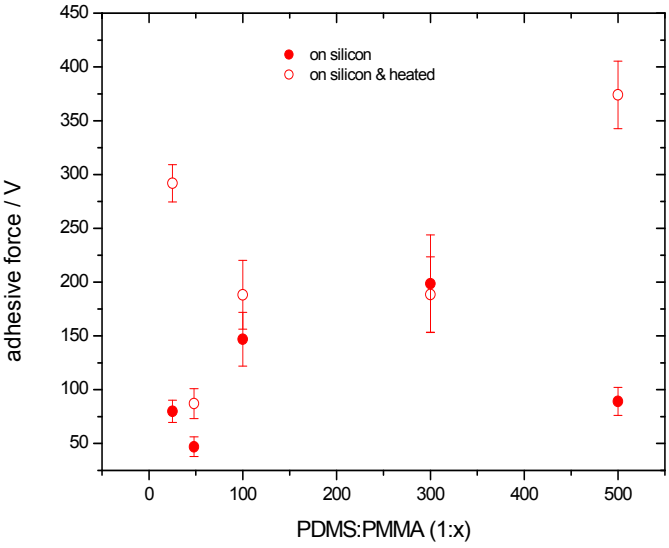

Figure 4.21: Change in surface polarity (as determined by the adhesion force) with increasing PMMA content.

4.4.3 PAS-FTIR spectroscopy

In PAS-FTIR, peak areas are relative to the amount of functional groups present if the analysis is carried out under the same conditions for each analysis. A ratio of the peaks gives relative concentrations of functional groups according to their chemical composition. This technique was used to investigate the degradation behaviour induced by corona treatment as well as to further investigate the PDMS surface segregation. FTIR data can indicate the presence of new or altered chemical groups after surface modification.

An analysis of the PAS-FTIR spectrum in Figure 4.22 gives us useful information by the characteristic IR absorption bands of PMMA-g-PDMS. Peak assignments for all of the functional groups have been made in Table 4.8 and Table 4.9.

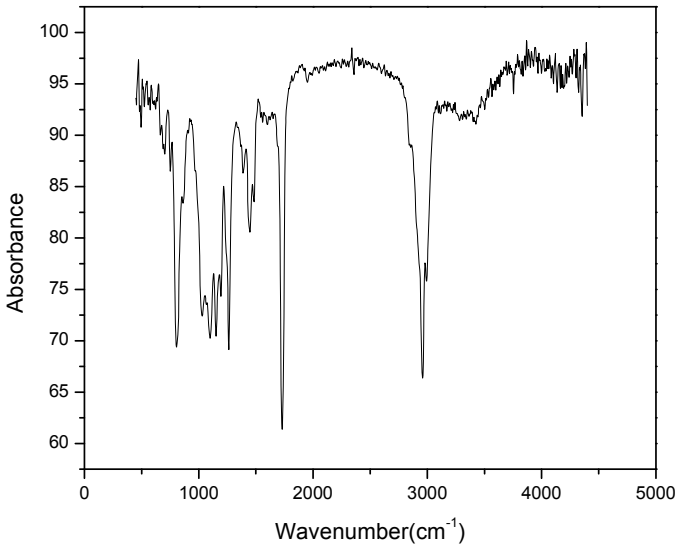

Figure 4.22: PAS-FTIR spectrum of PMMA-g-PDMS copolymer

Table 4.8: The characteristic IR absorption bands for PDMS[9,10]:

Wavenumber(cm^{-1})	Bond
3700-3200	OH
2962-2960	CH in methyl
1680-1740	C=O
1640	OH in H_2O
1440-1410	CH
1270-1255	Si-CH_3
1100-1000	Si-O-Si
870-850	$Si(CH_3)_3$

Table 4.9: The characteristic IR absorption bands for PMMA:

Wavenumber(cm^{-1})	Bond
2950	CH_3
1730	Ester carbonyl
1448	CH_2 stretch
1148	C-O-C

Sampling depth can be varied in PAS-FTIR analysis by varying the scan speed of the analysis. A decrease in scan speed would lead to a deeper penetration into the sample; resulting in the analysis of the bulk of the sample. A faster scan speed would lead to a scan on the surface of the sample. Therefore, by varying the scan speed, surface segregation of certain components of a copolymer can be detected. In this study the analysis were done at different scan speeds. The slowest scan speed was 0.05m/s, and thus the deepest penetration and 0.75m/s the fastest speed, and scans nearer to the surface. It is expected that the hydrophobic PDMS would migrate to the surface of the PMMA-g-PDMS and therefore the largest PDMS peaks are expected at the surface or higher speed scans. This expected trend can be observed in figure 4.23. The higher the scan speed, the larger the PDMS peaks is due to the fact that the sample is scanned closer to the surface of the sample as the scan speed increases.

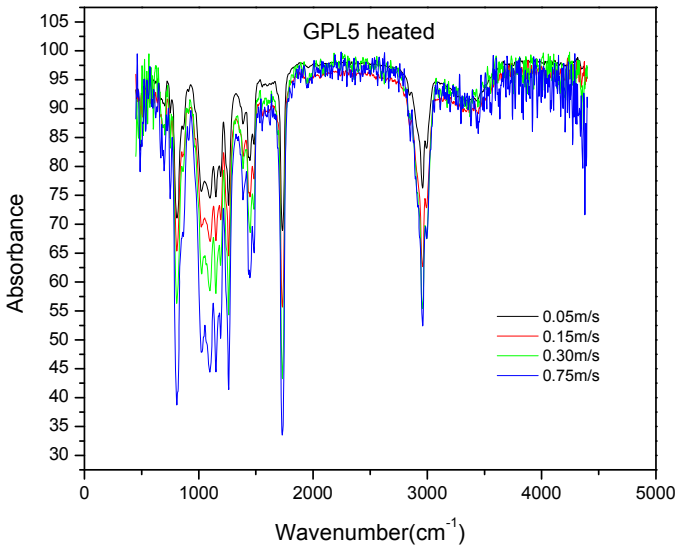

Figure 4.23: PAS-FTIR spectra of GPL5 (1:500 ratio of PDMS:PMMA with long macromonomer) heated, at different scan speeds.

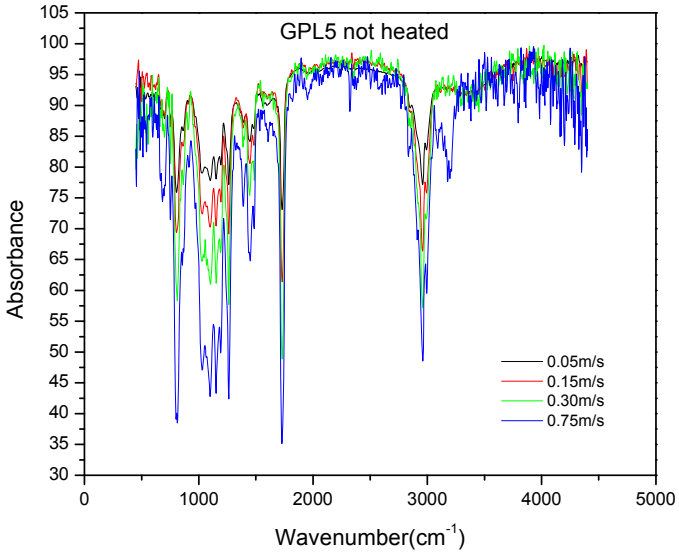

Figure 4.24: PAS-FTIR spectra of GPL5 (1:500 ratio of PDMS:PMMA with long macromonomer), at different scan speeds.

The expected trend of increasing PMMA:PDMS ratio with deeper penetration can be observed in Table 4.10. The PMMA:PDMS ratio was determined by integrating peaks

corresponding to PMMA and PDMS respectively. The two peaks that were compared were the peak at 850 cm^{-1} corresponding to PDMS and the peak at 1730 cm^{-1} corresponding to the ester carbonyl of PMMA. These peaks were integrated and relative peak areas were compared.

Table 4.10: PDMS:PMMA ratio of different graft copolymers determined by comparing peaks corresponding to PDMS and PMMA respectively.

GPL5 heated	PMMA	PDMS	PMMA/PDMS
0.75 m/s	1	1.07	0.9346
0.3 m/s	1.25	1	1.2500
0.15m/s	1.44	1	1.4400
0.05m/s	1.038	1	1.0380

GPL5 not heated	PMMA	PDMS	PMMA/PDMS
0.3 m/s	1.01	1	1.0100
0.15m/s	1.22	1	1.2200
0.05m/s	1.01	1	1.0100

GPM7 heated	PMMA	PDMS	PMMA/PDMS
0.75 m/s	1	1.257	0.7955
0.3 m/s	1.02	1	1.0200
0.15m/s	1.01	1	1.0100
0.05m/s	1	1.11	0.9009

GPM7 not heated	PMMA	PDMS	PMMA/PDMS
0.75 m/s	1	1.3649	0.7327
0.3 m/s	1	1.24	0.8065
0.15m/s	1.08	1	1.0800
0.05m/s	1	1.1	0.9091

GPM6 heated	PMMA	PDMS	PMMA/PDMS
0.75 m/s	1	2.28	0.4386
0.3 m/s	1.34	1	1.3400

It is known that there are drastic structural changes in the surface of the graft copolymer samples after corona treatment. FTIR data can indicate the presence of new or altered chemical groups. The change in the Si-O absorption bands can be traced, as this would change as the $(SiO)_x$ layer forms. Carbonyl peaks or hydroxyl groups can also form after chain scission. On pure PMDS compounds it is known that the glassy layer is obtained by modification of the PDMS backbone. The fact that this degradation layer formed, is so

surface specific, when compared to the bulk material, almost no chemical changes could be detected.

Table 4.11: PDMS:PMMA ratio of different graft copolymers after corona treatment determined by comparing peaks corresponding to PDMS and PMMA respectively.

GPL5 not heated	PMMA	PDMS	PMMA/Si-O-Si
0.3 m/s	1.01	1	1.0100
0.15m/s	1.22	1	1.2200
0.05m/s	1.01	1	1.0100
GPL5 corona	PMMA	PDMS	PMMA/Si-O-Si
0.75 m/s	1.11	1	1.1100
0.3 m/s	1.2	1	1.2000
GPM7 not heated	PMMA	PDMS	PMMA/Si-O-Si
0.75 m/s	1	1.3649	0.7327
0.3 m/s	1	1.24	0.8065
0.15m/s	1.08	1	1.0800
0.05m/s	1	1.1	0.9091
GPM7 corona	PMMA	PDMS	PMMA/Si-O-Si
0.75 m/s	1	1.71	0.5848
0.3 m/s	1	1.09	0.9174

Figure 4.25 is an overlay of GPM7 showing the traces before and after corona treatment. Small changes in the overlay of these untreated and corona treated films can be noticed. Only a few of the samples in table 4.11 showed an increase in PDMS ratio after corona treatment. This result is expected due to the development of the $(Si\text{-}O)_x$ glassy layer after corona treatment. Other possible degradation peaks such as hydroxyl groups (around 3300cm^{-1}) or carbonyls (around 1650-1700 cm^{-1}) could not be established due to concentration issues. Hillborg and Gedde[11] studied pure crosslinked PDMS after extended times of corona. They also found that the degradation is too surface specific to detect using FTIR techniques. The FTIR technique used in their study was ATR-FTIR and not PAS-FTIR. PAS-FTIR has an even larger sampling depth than ATR-FTIR. The estimated penetration depth of PAS is between 5-15 micrometers[12].

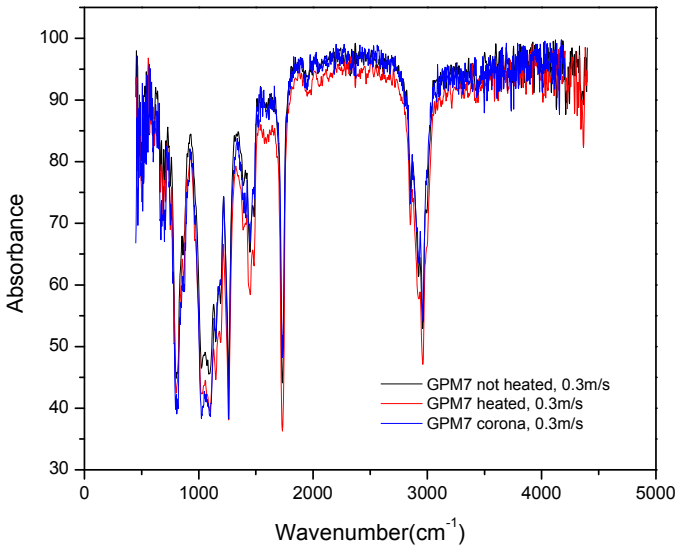

Figure 4.25: Differently treated samples of GPM7 run at a scan speed of 0.3m/s.

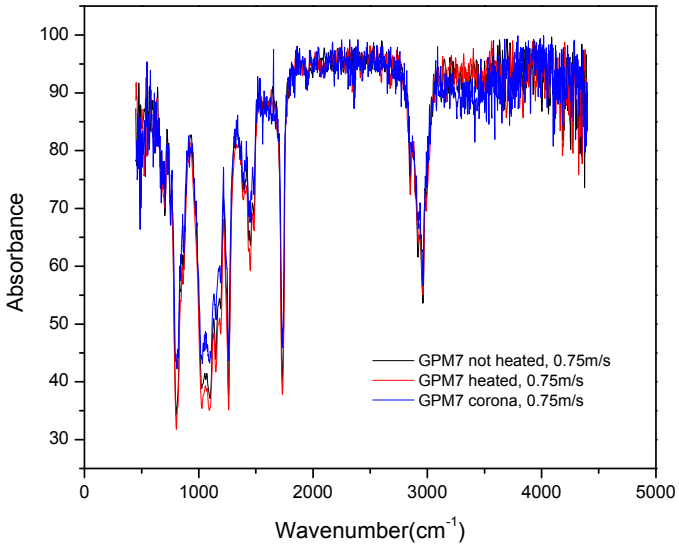

Figure 4.26: Differently treated samples of GPM7 run at a scan speed of 0.75m/s.

The surface changes are estimated to be only for the first few nanometers as estimated from slow positron beam results in section 4.4.4.

4.4.4 Slow positron beam analysis

Positron annihilation spectroscopy is a non-destructive technique for material characterisation. It presents useful information about defect properties of the material under study. Results in this study are presented in terms of a defect or S parameter. In polymers, a larger S-parameter indicates a larger free volume or defect parameter. This technique is used to investigate microstructural change at the molecular level at the early stage of material degradation[13].

Figure 4.27 shows the S-parameter profiles as a function of the positron implantation energy and the mean implantation depth for the various copolymer samples (made using the “short” PDMS macromonomer) as well as for a pure PDMS (crosslinked) and PMMA sample. As for most polymers, the S-parameter is low at the surface and increases as higher implantation depth until it reaches a maximum value[14]. This can be explained by the “back diffusion” of the positrons from the surface into the vacuum. The depth at which the S-parameter reaches its maximum value corresponds to the positron diffusion length in each polymer sample. In some cases there is a decrease in the S-parameter at higher implantation depth (for example the 1:25 and 1:300 samples). This is due to the positrons penetrating through the film and annihilating on the glass substrate. The depth at which there is a decrease in the S-parameter correlates to the thickness of the polymer films and as such has no significance in terms of the chemical or morphological nature of the polymer samples. The S-parameter profile of a pure PMMA film and a crosslinked PDMS sample are included in the figure for comparison purposes. It is necessary to use a crosslinked PDMS sample as PDMS has a very low Tg and as such the un-crosslinked polymer is a viscous liquid even at very high molecular masses.

The S-parameter depends largely on the free volume properties of a polymer surface and to a lesser extent on the chemical nature of the surface. A larger S-parameter corresponds to a larger free volume in the polymer. When comparing the S-parameter profiles in figure 4.27, of the pure PDMS and pure PMMA samples at the maximum value, it can be seen that the PDMS has a much higher S-parameter value than the PMMA. This is expected since the PDMS has a Tg of -127˚C and PMMA has a Tg of 110°C and therefore the PDMS has a larger free volume at the measurement temperature.

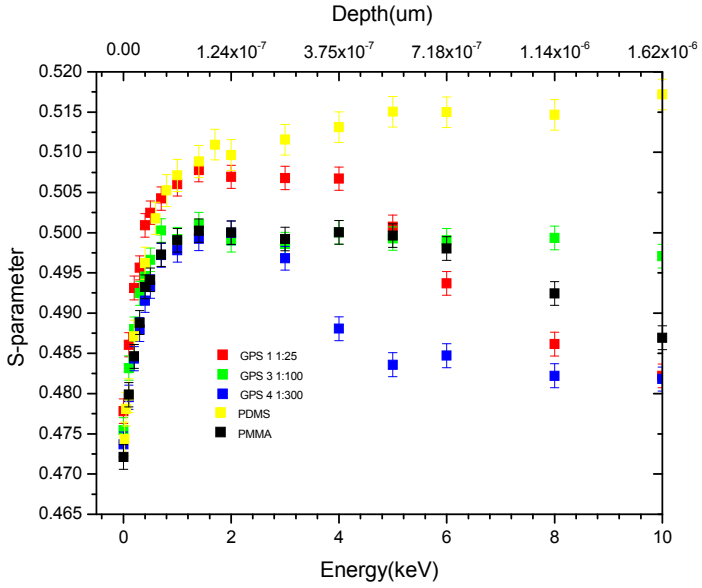

Figure 4.27: S-parameter as a function of positron implantation energy and mean implantation depth for the graft copolymers, made with the “short macromonomer”. The values in the legend refer to the ratio of the PDMS to PMMA in the copolymer feed.

The S-parameter profile of the 1:25 ratio copolymer (high PDMS branch content polymer) follows closely that of the pure PDMS compound at low implantation energies, but reaches a slightly lower S-parameter value at the plateau. For the copolymers with progressively lesser amounts of the PDMS graft there is a progressive decrease in the S-parameter at the surface until the lowest graft content sample has an S-parameter profile that matches closely that of pure PMMA. This progressive decrease in the S-parameter as a function of the graft PDMS content is due to the PDMS component in the copolymers and may indicate the preferential surface segregation of the PDMS component in the polymers.

Figure 4.28 shows a similar S parameter profile of the graft copolymers as a function of the PDMS graft length for the same PDMS:PMMA ratio of 1:100. Once again the decrease in the S-parameter value at higher positron implantation energies for the “long” PDMS grafts corresponds to the positron penetrating the film and annihilating on the glass substrate. Once again there is a correlation between the amount of PDMS (in this case due to the longer graft lengths) and the maximum S-parameter value measured. Again there is a progressive decrease in the S-parameter with a lower PDMS content

and this may be due to the preferential surface segregation of the PDMS component in the copolymer. This is supported by the fact the measured S-parameter at the very low positron implantation depth is considerably higher for the long and medium graft length copolymers.

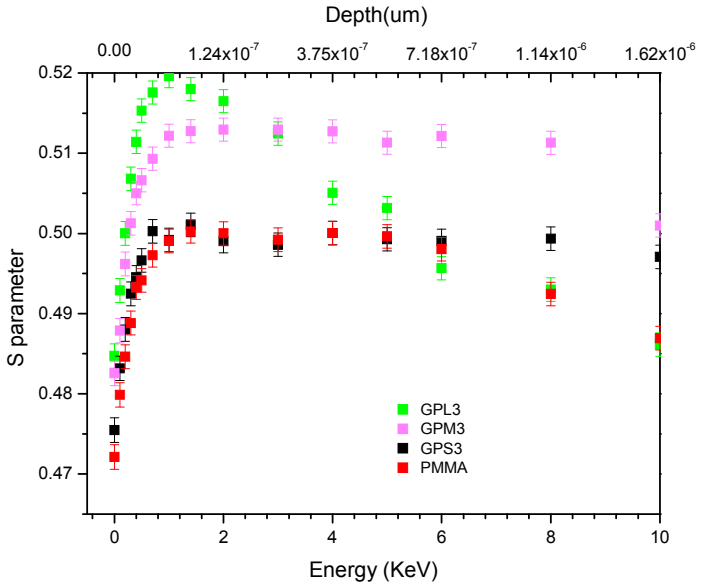

Figure 4.28: S-parameter profile as a function of the positron implantation energy and mean implantation depth as a function of the macromonomer length.

Figure 4.29 to Figure 4.31 show the S-parameter profiles of several of the copolymers before and after exposure to corona treatment. In all cases it can be seen that the corona treatment has a drastic impact on the measured S-parameter profile of the polymer.

There is a large drop in the S-parameter near the surface in all of the polymers after corona exposure. A similar decrease was observed by Mallon *et al.*[15] after the exposure of crosslinked pure PDMS samples to corona treatment. This decrease was observed to be due to the degradation of the PDMS to form a SiO_x type degradation layer on the surface of the polymer. In the current study a similar decrease is observed, but the levelling off of the S-parameter observed in the very near surface region of the pure PDMS compounds, is not as apparent in the graft copolymer. There is, however, some indication that there is a levelling of in the very near surface region in the 1:25, 1:100

and 1:300 short samples. This may be due to a similar formation of a SiO_x degradation layer as that observed in the pure PDMS compounds.

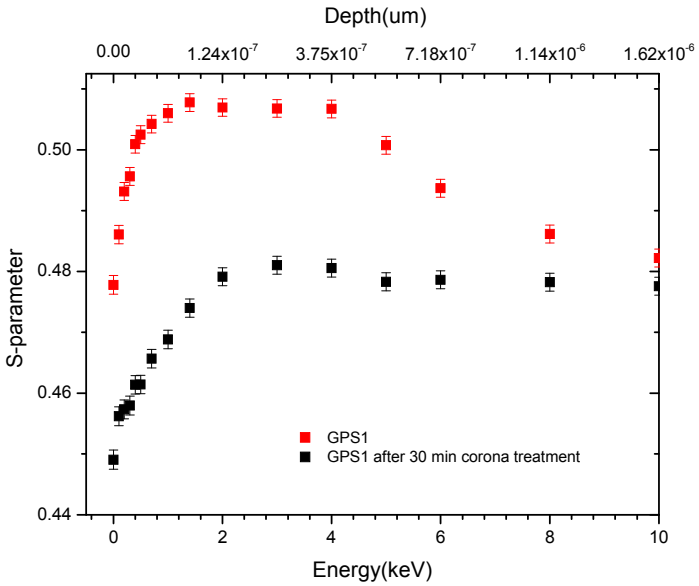

Figure 4.29: S parameter profile of the virgin and 30 minute corona treated 1:25 graft copolymers made with the “short” PDMS macromonomer.

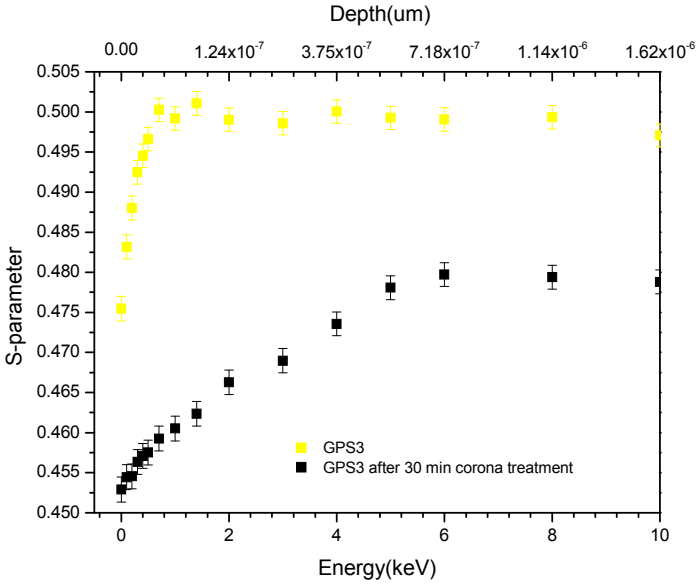

Figure 4.30: S parameter profile of the virgin and 30 minute corona treated 1:100 graft copolymers made with the “short” PDMS macromonomer.

Despite the very large changes observed in the S-parameter profiles the changes after corona degradation are very surface specific. It is estimated that the dramatic changes occur in the first 3-20 nm of the surface as indicated by the 'levelling off' of the S-parameter. The changes in the rest of the S-parameter profile at larger depths are a result of the fact that at higher depth (implantation energies) the implanted positron must move through this degradation layer. The higher density and chemical modification results in a larger fraction of positrons annihilation in the surface layer after the corona exposure.

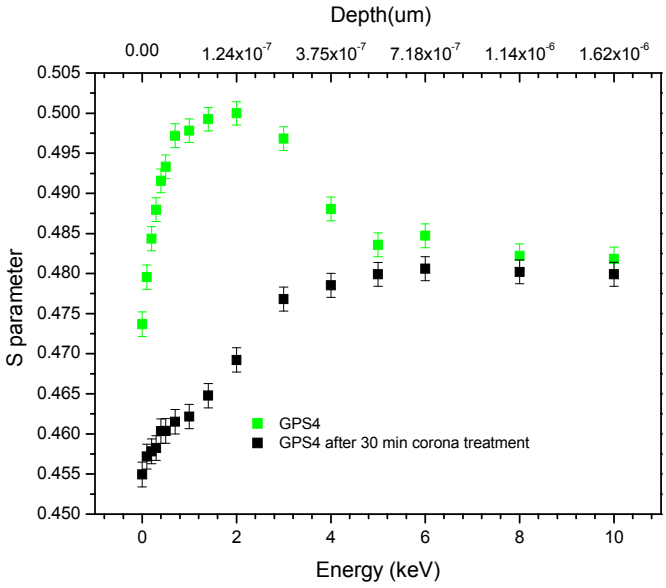

Figure 4.31: S parameter profile of the virgin and 30 minute corona treated 1:300 graft copolymers made with the "short" PDMS macromacromonomer

4.5 References

(1) Smith, S. D.; DeSimone, J. M.; Huang, H.; York, G.; Dwight, D. W.; Wilkes, G. L.; McGrath, J. E. *Macromolecules* **1992**, *25*, 2575-2581.

(2) *Encyclopedia of Polymer Science*, *2*, 1-11.

(3) Elkins, C. L.; Long, T. E. *Macromolecules* **2004**, *37*, 6657-6659.

(4) Vadala, M. L.; Rutnakornpituk, M.; Zalich, M. A.; St Pierre, T. G.; Riffle, J. S. *Polymer* **2994**, *45*, 7449-7461.

(5) Graef, S. M.; Van Zyl, A. J. P.; Sanderson, R. D.; Klumperman, B.; Pasch, H. *J. Appl. Polym. Sci.* **2003**, *88*, 2530-2538.

(6) Lee, Y.; Akiba, I.; Akiyama, S. *J. Appl. Polym. Sci.* **2003**, *87*, 375-380.

(7) Bayley, G.; Mallon, P. E. *Polym. Eng. Sci.* **2007**, *article in press*.

(8) Kim, J.; Chaudhury, M. K.; Owen, M. J.; Orbek, T. *J. Colloid Interface Sci.* **2001**, *244*, 200-207.

(9) Yoshimura, N.; Kumgai, S.; Nishimura, S. *IEEE. Trans. Diel. Elect. Insul.* **1999**, *6*, 632-649.

(10) Kim, S. H.; Cherney, E. A.; Hackham, R.; Rutherford, K. G. *IEEE. Trans. Diel. Elect. Insul.* **1994**, *1*, 106-122.

(11) Hillborg, H.; Sandelin, M.; Gedde, U. W. *Polymer* **2001**, *42*, 7349-7362.

(12) Gonon, L.; Mallegol, J.; Commereuc, S.; Verney, V. *Vib. Spectrosc* **2001**, *26*, 43-49.

(13) Mallon, P. E. In *Chapter 10: Application to Polymers. Principles and Applications of Positron and Postronium Chemistry.*; Jean, Y. C.; Mallon, P. E.; Schrader, D. M., Eds.; World Scientific Publishing: Singapore, 2003.

(14) Jean, Y. C.; Mallon, P. E.; Zhang, R.; Chen, H.; Wu, Y.; Li, Y.; Zhang, J. In *Chapter 11: Applications of Slow Positrons to Polymeric Surfaces and Coatings. Principles and Applications of Positron and Positronium Chemistry.*; Jean, Y. C.; Mallon, P. E.; Schrader, D. M., Eds.; World Scientific Publishing: Singapore, 2003.

(15) Mallon, P. E.; Berhane, T. A.; Greyling, C. J.; Vosloo, W. L.; Chen, H.; Jean, Y. C. *Mater. Sci. Forum* **2004**, *445-446*, 322-324.

Conclusions and Recommendations

5.1 Conclusions

The summarised conclusions of this research study are as follows:

- The successful evaluation of the synthesis of PDMS-MA macromonomers via two different techniques.
  - The living anionic polymerisation of the D_3 monomer and functional termination with a chlorosilane derivative of allyl methacrylate to afford a methacryloxy-functionalised PDMS macromonomer was found a successful technique to form narrowly dispersed macromonomer chains.
  - The functionalisation of a monohydroxy-terminated PDMS to form the PDMS-MA macromonomer was found to be time-consuming and not very successful.
- The successful synthesis of PMMA-graft-PDMS copolymers via a conventional free radical reaction. Anionically synthesised and commercial PDMS-MA macromonomers were copolymerised with MMA using the grafting through or macromonomer technique to produce graft copolymers with various chemical compositions. The ratio of MMA to PDMS was varied as well as the PDMS side chain length.
- Successful development of a GEC profile, allowing the monitoring of PDMS macromonomer before and after extraction.
- Succesfull two dimensional evaluation of the graft copolymers coupling GEC to SEC. This allows monitoring of graft copolymer as well as a varying amount of PMMA homopolymer formation. These analyses can be highlighted due to the unusual two-dimensional combination. The two dimensional analysis shows that for the longer macromonomer series some degree of PMMA homopolymerisation is observed while this is not evident for the shorter series. The two dimensional analysis also shows that the higher graft content molecules generally have a lower molar mass.

- This study shows the first evidence for hydrophobic loss and recovery after corona treatment for PDMS hybrid materials by static contact angle measurements before and after corona treatment.
- The successful surface segregation of PDMS is shown by AFM and PAS-FTIR studies.
- This study shows evidence for the formation of a silica like (SiO_x) layer after corona treatment in PDMS based hybrid materials and the thickness of this layer was estimated using the depth profiling capabilities of the slow positron beam technique.

5.2 Recommendations

More attention needs to be paid to the studying of the degradation mechanism after corona treatment. It is clear that this is a true surface phenomenon from the positron data, which makes analysis difficult due to the small concentrations of degradation species compared to that of the bulk material. The PAS-FTIR data showed almost no change in absorption bands after corona treatment or no new absorption bands could be detected after corona treatment illustrating that the concentration of degradation species are too small to be detected. A possible way to increase the amount of degradation species is by increasing the surface area. This could be achieved by spinning nano-fibres of the polymer material and corona treating these surfaces. The production of nanofibers would also potentially be a means of exploiting the preferential surface segregation in these copolymers.

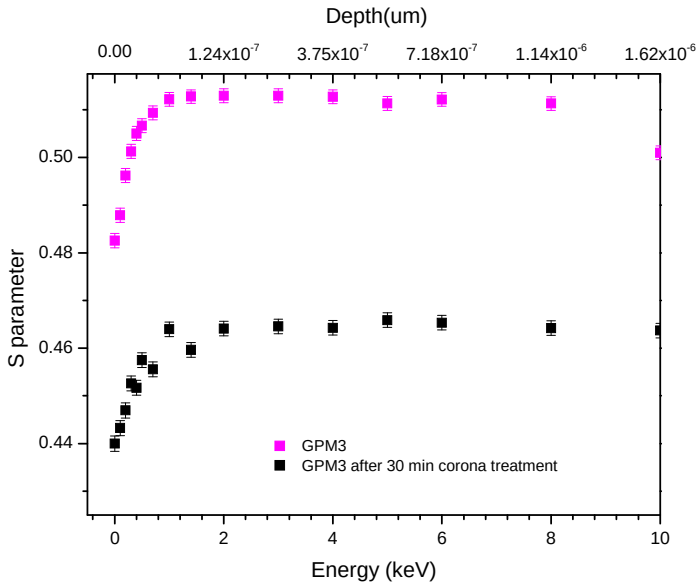

Figure A.1: S parameter profile of the virgin and 30 minute corona treated 1:100 graft copolymers made with the “medium” PDMS macromonomer (GPM3).

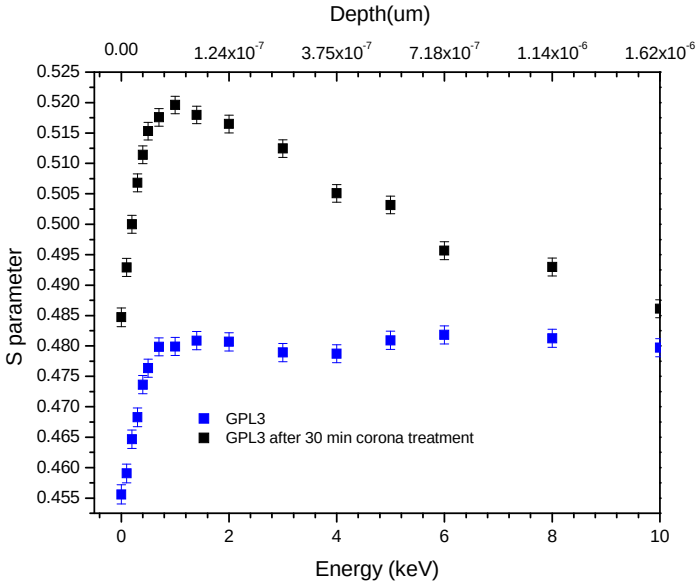

Figure A.2: S parameter profile of the virgin and 30 minute corona treated 1:100 graft copolymers made with the “long” PDMS macromonomer (GPL3).

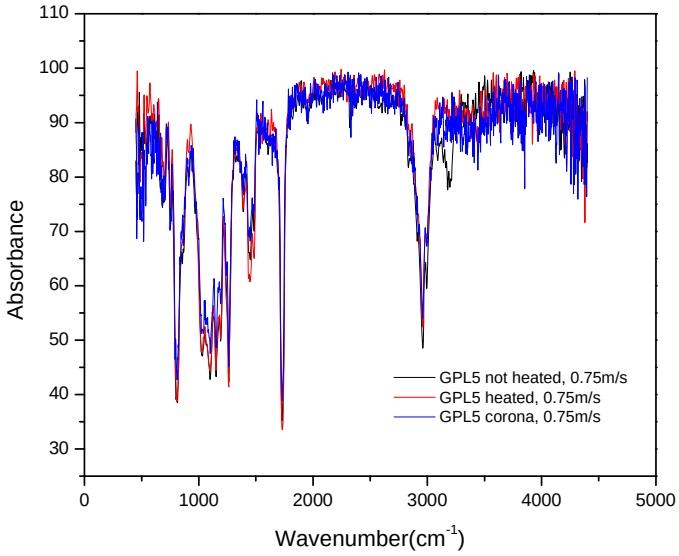

Figure B.1: PAS-FTIR overlay of differently treated samples of GPL5 run at a scan speed of 0.75m/s.

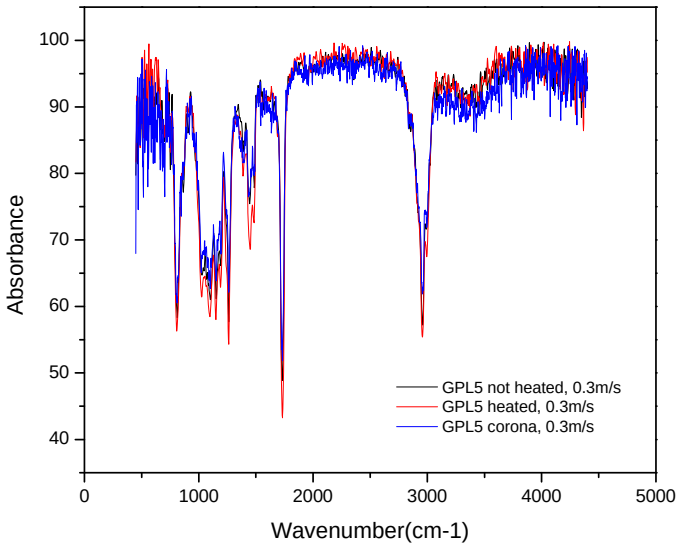

Figure B.2: PAS-FTIR overlay of differently treated samples of GPL5 run at a scan speed of 0.3m/s.